

UC Santa Cruz

UC Santa Cruz Previously Published Works

Title

Differential effects of nitrate, ammonium, and urea as N sources for microbial communities in the North Pacific Ocean

Permalink

<https://escholarship.org/uc/item/4b92d1kz>

Journal

LIMNOLOGY AND OCEANOGRAPHY, 62(6)

ISSN

0024-3590

Authors

Shilova, IN
Mills, MM
Robidart, JC
[et al.](#)

Publication Date

2017-11-01

DOI

10.1002/lno.10590

Peer reviewed

1 **Title**

2 Differential effects of nitrate, ammonium and urea as N sources for microbial communities in the
3 North Pacific Ocean

4

5 **Authors**

6 ¹Shilova IN^a, ²Mills MM^a, ³Robidart JC, ¹Turk-Kubo KA, ⁴Björkman KM, ¹Kolber Z, ⁵Rapp I.,
7 ²van Dijken GL, ⁴Church MJ[†], ²Arrigo KR, ⁵Achterberg EP, ¹Zehr JP*

8

9 ¹University of California Santa Cruz, CA, USA; ²Stanford University, Stanford, CA, USA;
10 ³National Oceanography Centre, Southampton, UK; ⁴University of Hawaii at Manoa, Honolulu,
11 HI, USA; ⁵GEOMAR Helmholtz Centre for Ocean Research, Kiel, Germany

12

13 ^aEqual contribution

14 [†] Present address: Flathead Lake Biological Station, University of Montana, Polson, MT, USA

15

16 *Correspondence: Department of Ocean Sciences, University of California Santa Cruz, 1156
17 High Street, Santa Cruz, CA 95064; Email: zehrj@ucsc.edu

18

19 Running title: N effects on microbial communities

20

21 Keywords: nitrogen, phytoplankton, microbial community, *Prochlorococcus*, *Synechococcus*,
22 urea, nitrate, ammonium, iron, nutrient limitation, North Pacific, oligotyping

23

24 **Abstract**

25 Nitrogen (N) is the major limiting nutrient for phytoplankton growth and productivity in large
26 parts of the world's oceans. Differential preferences for specific N substrates may be important
27 in controlling phytoplankton community composition. To date, there is limited information on
28 how specific N substrates influence the composition of naturally occurring microbial
29 communities. We investigated the effect of nitrate (NO_3^-), ammonium (NH_4^+) and urea on
30 microbial and phytoplankton community composition (cell abundances and 16S rRNA gene
31 profiling) and functioning (photosynthetic activity, carbon fixation rates) in the oligotrophic
32 waters of the North Pacific Ocean. All N substrates tested significantly stimulated phytoplankton
33 growth and productivity. Urea resulted in the greatest (>300%) increases in chlorophyll *a* (<0.06
34 and $\sim 0.19 \mu\text{g L}^{-1}$ in the control and urea addition, respectively) and productivity (<0.4 and ~ 1.4
35 $\mu\text{mol C L}^{-1} \text{d}^{-1}$ in the control and urea addition, respectively) at two experimental stations, largely
36 due to increased abundances of *Prochlorococcus* (Cyanobacteria). Two abundant clades of
37 *Prochlorococcus*, High Light I and II, demonstrated similar responses to urea, suggesting this
38 substrate is likely an important N source for natural *Prochlorococcus* populations. In contrast,
39 the heterotrophic community composition changed most in response to NH_4^+ . Finally, the time
40 and magnitude of response to N amendments varied with geographic location, likely due to
41 differences in microbial community composition and their nutrient status. Our results provide
42 support for the hypothesis that changes in N supply would likely favor specific populations of
43 phytoplankton in different oceanic regions and thus, affect both biogeochemical cycles and
44 ecological processes.

45

46

47 **Introduction**

48 Nitrogen (N) is a major component of cell constituents, including proteins and nucleic
49 acids, and is considered the primary limiting element for phytoplankton growth and
50 photosynthetic carbon fixation in oligotrophic oceans (Eppley et al. 1977; Graziano et al. 1996;
51 Mills et al. 2004; Moore et al. 2013). While there is an intricate balance among iron (Fe),
52 phosphorus (P) and N in shaping microbial communities in the marine environment, nutrient
53 enrichment experiments have demonstrated that the availability of N alone can stimulate growth
54 of phytoplankton and affect heterotrophic communities in the oligotrophic ocean (Mills et al.
55 2004, 2008; Bonnet et al. 2008; Davey et al. 2008; Moore et al. 2008; Ortega-Retuerta et al.
56 2012).

57 N actively cycles in the upper ocean where sunlight provides energy that rapidly fuels
58 production and consumption of N compounds. The major forms of N in the surface ocean
59 include dinitrogen gas (N_2), ammonium (NH_4^+), nitrate (NO_3^-), nitrite (NO_2^-) and dissolved
60 organic N (DON). N_2 fixation can account for 40-50% of net community production in the North
61 Pacific Subtropical Gyre (NPSG) (Böttjer et al. 2016), however, net community production in
62 this ecosystem is less than 10% of gross primary production (Quay et al. 2010). Although
63 abundant, the bulk of the DON pool, except urea, amino acids and nucleotides, generally do not
64 appear readily bioavailable and are believed to be minor sources of N for most phytoplankton
65 (Aluwihare and Meador 2008; Mulholland and Lomas 2008). The major fixed N sources (NH_4^+ ,
66 NO_3^- , and urea) have different sources and rates of production and turnover. Regeneration by
67 heterotrophic bacteria, and excretion and release by zooplankton, are the major natural sources of
68 NH_4^+ and urea in the upper ocean (Corner and Newell 1967; Mayzaud et al. 1973; Mitamura and
69 Saijo 1981; Bidigare 1983; Hansell and Goering 1989; Bronk et al. 1998). Regenerated

70 production supported by this rapidly recycled N accounts for over 90% of gross primary
71 production in the oligotrophic oceans (Eppley and Peterson 1979). NO_3^- is supplied to the
72 euphotic zone predominately via mixing or upwelling of sub-euphotic zone waters with
73 additional contributions derived from nitrification within the euphotic zone (Dore and Karl 1996;
74 Yool et al. 2007) and atmospheric deposition (Duce et al. 2008). N from sources external to the
75 surface ocean supports “new” production, which balances N export losses due to sinking to the
76 deep ocean (Dugdale and Goering 1967). New N is also introduced through N_2 fixation carried
77 out by diazotrophs, a small subset of the marine microbial community (Dugdale and Goering
78 1967; Zehr and Kudela 2011). Recycling of diazotroph organic matter transfers this new N to the
79 dissolved pool as DON (e.g. amino acids and urea) and/or NH_4^+ where it can be used to fuel
80 primary production (Montoya et al. 2002; Zehr and Kudela 2011). Thus, the chemical form of N
81 is an important factor in the functioning of ocean ecosystems.

82 Microbial communities that utilize dissolved N in oligotrophic oceans are diverse, but are
83 comprised largely of cyanobacteria (*Prochlorococcus* and *Synechococcus*), diatoms, eukaryotic
84 picoplankton (for example, prymnesiophytes and pelagophytes) and a variety of heterotrophic
85 bacteria (including *Pelagibacter ubique*) and Archaea (Waterbury et al. 1979; Chisholm et al.
86 1988; DuRand et al. 2001; Karner et al. 2001; Morris et al. 2002; Worden et al. 2004). These
87 microorganisms have a variety of N assimilation strategies that differ in the rates of N uptake and
88 assimilation, regulation of N metabolism, and their abilities to use different N forms. For
89 example, N-limited Low Light (LL) *Prochlorococcus* strains appear unable to grow on NO_3^-
90 (Moore et al. 2002), while some strains of the High Light (HL) ecotypes are able to assimilate
91 NO_3^- , although at reduced rates of growth relative to other substrates (e.g. NH_4^+ , Martiny et al.
92 2009; Berube et al. 2015). Many marine microorganisms use NO_3^- as a source of N, including

93 diatoms and *Synechococcus*, as well as some heterotrophic bacteria (Allen et al. 2001, 2006;
94 Casey et al. 2007; Collier et al. 2012). Isotopic analyses suggest that eukaryotic phytoplankton
95 smaller than 30 μm in the Sargasso Sea acquire a major fraction of their N demand from NO_3^-
96 (Fawcett et al. 2011). The assimilation of urea by phototrophic and heterotrophic marine
97 microorganisms is common across numerous phylogenetic groups and ecological niches
98 (McCarthy et al. 1972a, b; Hallam et al. 2006; Baker et al. 2009; Collier et al. 2009; review by
99 Solomon et al. 2010). Many *Prochlorococcus* strains and all tested *Synechococcus* strains can
100 utilize urea, yet this N substrate supports different growth rates within each genus (Moore et al.
101 2002). Moreover, rates of urea uptake and assimilation in natural microbial populations appear
102 comparable to those of NH_4^+ (Sahlsten 1987; Price and Harrison 1988), although rates differ
103 among phytoplankton taxa (Lomas and Glibert, 2000; Moore et al. 2002; Fan et al. 2003).
104 Despite the accumulated knowledge about N utilization by marine microorganisms, taxon-
105 specific preferences and utilization efficiencies for different N species is still ambiguous,
106 especially in the oligotrophic open ocean.

107 The form and supply of different N substrates are important controls on microbial
108 community composition. Understanding the effect of different N forms is critical because N
109 supply to the surface oceans will likely change due to greater stratification caused by climate
110 change (Gruber and Galloway 2008; Capotondi et al. 2012; Kim et al. 2014), and the projected
111 increase in atmospheric anthropogenic N deposition (Duce et al. 2008). We performed nutrient
112 enrichment experiments to determine the functional and taxonomic responses in microbial
113 communities to different N forms and whether the response varies depending on the nutrient
114 status (mesotrophic versus oligotrophic) in the North Pacific Ocean. The measured functional
115 responses included CO_2 fixation rates and changes in chlorophyll *a* (Chl *a*) and photosynthetic

116 parameters, while the taxonomic responses were assessed by quantifying the abundance of major
117 phytoplankton groups and heterotrophic bacteria as well as assessing relative shifts in
118 cyanobacterial and heterotrophic community composition based on 16S rRNA gene sequencing.

119

120 **Materials and Methods**

121 *Nutrient amendments experiments*

122 Experiments were conducted in August of 2014 during the Nitrogen Effects on Marine
123 microOrganisms cruise (NEMO, R/V *New Horizon*) at two sites in the North Pacific Ocean: one
124 within the western part of transitional zone of California Current System (CCS; Station 38,
125 hereafter referred to as TZ), and one in the oligotrophic NPSG (Station 52, hereafter referred to
126 as GY: Fig. 1). The TZ site was in an anticyclonic eddy, based on the sea surface height anomaly
127 (Fig. 1b). The two sites were chosen based on a priori assumptions of nutrient limitation of
128 primary productivity at each site. The availability of Fe can play an important role in controlling
129 phytoplankton growth in the CCS (Biller and Bruland 2014). In contrast, N was assumed to be
130 limiting primary productivity in the NPSG. All experiments were undertaken using strict trace-
131 metal clean techniques (Mills et al. 2004) during the preparation and sampling of the
132 experiments. Water at each station was collected from 25 m depth using a towed fish with Teflon
133 diaphragm pump. The water was pumped gently into a 40 L carboy in a trace-metal clean
134 laboratory van. This allowed mixing of the seawater before it was distributed into incubation
135 bottles. Seawater was subsampled into 4 L polycarbonate bottles (Thermo Scientific™
136 Nalgene™) that had been acid-washed and, prior to the experiment, rinsed thoroughly with
137 seawater at the site of each experiment. The bottles used in the first experiment were acid-rinsed
138 and reused for the same treatments in the second experiment. In the TZ site experiment, triplicate

139 incubation bottles were amended with either NO_3^- (final concentration $5.0 \mu\text{mol L}^{-1}$), NH_4^+ (final
140 concentration $5.0 \mu\text{mol L}^{-1}$), urea (final concentration $5.0 \mu\text{mol N L}^{-1}$), $0.2 \mu\text{m}$ pre-filtered deep
141 (600 m) seawater (FDW) (12.5% of total volume, equivalent to $\sim 5 \mu\text{mol L}^{-1} \text{NO}_3^-$ addition),
142 Fe^{3+} (final concentration 2 nmol L^{-1}) or a combined treatment containing NO_3^- and Fe^{3+} (final
143 concentrations of $5 \mu\text{mol L}^{-1}$ and 2 nmol L^{-1} , respectively). The Fe and Fe+ NO_3^- treatments were
144 used to test for Fe and Fe+ NO_3^- co-limitation. The GY experiment was similar in design with the
145 exception that all N compounds were added to achieve a final concentration of $2.5 \mu\text{mol N L}^{-1}$,
146 and 6% of total volume of FDW was added (an approximately $2.5 \mu\text{mol L}^{-1} \text{NO}_3^-$ addition). The
147 N additions in the TZ experiment were higher than in the GY experiment based on previous
148 work in the CCS by Biller and Bruland (2014) who measured residual NO_3^- concentrations in the
149 transitional zone of CCS ranging from $5\text{-}15 \mu\text{mol L}^{-1}$, while residual NO_3^- at the GY was
150 negligible ($<10 \text{ nmol L}^{-1}$). In both experiments, the Controls consisted of triplicate bottles filled
151 with unamended seawater from the respective station and depth. The Controls were incubated
152 and processed in the same manner as the experimental treatments. All nutrient additions were
153 undertaken in a laminar flow hood. The nutrient solutions, except the Fe solution, were passed
154 through Chelex100 to minimize trace metal contamination. Purity controls were measured for all
155 stocks to ensure the absence of contamination (i.e., Fe stocks did not contain dissolved N, N
156 stocks did not contain Fe, and individual N stocks were not contaminated with other N species).
157 Incubation bottles were placed in a flow-through surface seawater incubator, to achieve surface
158 ocean temperatures during the experiment, with neutral screening to attenuate incident light to
159 approximately 35% of the surface solar irradiance. The setup and samplings of the setup (T0),
160 and at 24 (T24) and 48 (T48) hrs after the start of the incubation were undertaken before dawn.
161 Rates of primary productivity and concentrations of Chl *a* and nutrients were measured in

162 samples immediately after the nutrient amendments (T0) and at T48. Samples for
163 photophysiological parameters, cell abundance, and microbial community composition were
164 collected prior to the nutrient amendments (T0), at T24, and T48.

165

166 *Nutrient analysis*

167 Samples for subsequent analyses of nutrient concentrations were collected in acid-
168 washed, sample rinsed polyethylene bottles and stored frozen at -20°C until analyzed (Dore et al.
169 1996). $\text{NO}_3^- + \text{NO}_2^-$, soluble reactive phosphorus (SRP) and $\text{Si}(\text{OH})_4$ concentrations ($\mu\text{mol L}^{-1}$)
170 were determined using a segmented flow continuous flow automated nutrient analyzer (SEAL
171 Analytical - AA3) using standard colorimetric techniques (Strickland and Parson, 1972).
172 Accuracy of each analysis was checked using WAKO the International Cooperative Study of the
173 Kuroshio and Adjacent Regions (CSK) and Ocean Scientific International Ltd. (OSIL) reference
174 materials. $\text{NO}_3^- + \text{NO}_2^-$ concentrations $< 500 \text{ nmol L}^{-1}$ were determined using the high-sensitivity
175 chemiluminescence technique (Garside 1982; Dore and Karl 1996) with a detection limit of 1
176 nmol L^{-1} . NH_4^+ samples were measured using the SEAL AA3 coupled with a 2 m liquid
177 waveguide capillary cell, employing indophenol blue chemistry (Li et al. 2005; Zhu et al. 2014).
178 The limit of detection for this method is 4 nmol L^{-1} .

179 Samples for subsequent analyses of trace metal concentrations were collected using an
180 acid-cleaned hose (polyvinyl chloride, PVC) attached to a plastic-coated steel cable and lowered
181 to the desired collection depth (25 m). Water was pumped to the surface using a Teflon bellows
182 pump (Almatec A15) and transferred, entirely enclosed, into a trace-metal clean sampling
183 container located in an on-deck trace-metal clean lab. Samples for the determination of dissolved
184 Fe concentrations were filtered through a $0.2 \mu\text{m}$ Sartobran 300 capsule filter (Sartobran 300,

185 Sartorius), collected in acid-cleaned 125 mL low density polyethylene (LDPE, Nalgene) bottles,
186 and immediately acidified with 150 μL hydrochloric acid ($\sim 11 \text{ mol L}^{-1}$ HCl, OPTIMA grade,
187 Fisher Scientific) to a final pH of 1.9. Dissolved Fe samples from the incubation experiments
188 were collected at T0 and T48. The samples were filtered using 0.45 μm polycarbonate membrane
189 filters (Millipore) mounted in an acid cleaned filter holder (Swinnex, Millipore), acidified to pH
190 1.9. and analyzed on-board ship using flow injection analysis (FIA). Dissolved Fe was
191 determined on-board the ship using luminol chemiluminescence by flow injection analysis (FIA)
192 following Obata et al. (1993). The FIA system was equipped with a Toyopearl AF Chelate 650M
193 resin. Sample concentrations were determined by standard addition and were verified by
194 analyzing ‘Sampling and Analysis of Fe (SAFe)’ reference seawater with each analytical run.
195 Our results for the reference seawater were in good agreement with the consensus values for
196 SAFe S: $0.090 \pm 0.008 \text{ nmol L}^{-1}$ (n=2) and SAFe D2: $1.043 \pm 0.004 \text{ nmol L}^{-1}$ (n=2). The
197 precision of the method varied between 4 - 8% (1 SD) and was determined by analyzing internal
198 reference seawater after every 10 samples. The blank of the FIA method was $0.028 \pm 0.010 \text{ nmol}$
199 L^{-1} (n=12) and the limit of detection (LOD) determined by the product of the blank and three
200 times standard deviation of the blank was $0.058 \text{ nmol L}^{-1}$.

201

202 *Chlorophyll a*

203 Subsamples (300 or 400 mL) were collected from each of the triplicate bottles and
204 filtered through 25 mm diameter glass fiber filters (GF/F, Whatman). Filters were placed in 5 mL
205 of 90% acetone and extracted in the dark at 2°C for 24 hrs. Samples were equilibrated to room
206 temperature before measurement. Fluorescence at 685 nm was measured using a Turner Designs

207 TD-700 Field Fluorometer, calibrated with a Chl *a* standard (Sigma-Aldrich, C6144) dissolved in
208 90% acetone using the Welschmeyer (1994) filter setup.

209

210 *¹⁴C-based primary productivity*

211 Primary productivity (PP) was determined using ¹⁴C-labelled bicarbonate as a tracer for
212 net inorganic carbon fixation (Steeman-Nielsen 1952). A subsample from each treatment bottle
213 was collected into acid-cleaned, sample-rinsed 75 mL polycarbonate bottles and spiked with ¹⁴C-
214 bicarbonate to achieve a final activity of approximately 250 $\mu\text{Ci L}^{-1}$ (or 9.3 MBq L^{-1} , MP
215 Biomedical #017441H). The bottles were incubated from dawn to dusk in the same on-deck
216 incubator previously described. At the end of the daylight period, the entire sample volume was
217 filtered through a 25 mm GF/F. The filters were placed into 20 mL borosilicate scintillation
218 vials, acidified (1 mL, 2 mol L^{-1} hydrochloric acid) and vented for 24 hrs prior to the addition of
219 scintillation cocktail (Ultima Gold LLT, Perkin-Elmer). Radioactivity was determined by liquid
220 scintillation counting. Subsamples (250 μL) for total ¹⁴C-radioactivity were collected from each
221 incubation bottle and fixed in phenethylamine (Sigma-Aldrich #407267). Rates of carbon
222 fixation are expressed as $\mu\text{mol C L}^{-1} \text{d}^{-1}$.

223

224 *Active fluorescence*

225 Fast Repetition Rate Fluorometry (FRRF) was utilized to evaluate possible changes in
226 photophysiology in response to the availability of different N and Fe substrates, as described in
227 Kolber et al. (1998). The FRRF instrument was operated with multiple excitation wavelengths
228 (450 nm, 470 nm, 505 nm, and 530 nm) that allowed for the rapid assessment of photosystem II
229 physiology in different groups of phytoplankton. Samples (500 mL) were first dark adapted (20

230 min) before conducting fluorescence measurements. Fluorescence transients were acquired in
231 samples that were continuously recirculated through the instrument sample chamber. The sample
232 chamber was exposed to FRRF excitation protocol composed of a series of microsecond-long
233 flashlets of controlled excitation power. The saturation phase of the excitation was comprised of
234 100 flashlets at 2.5 microsecond intervals. With the pulse excitation power of 30,000 to 50,000
235 $\mu\text{mol quanta m}^{-2} \text{ s}^{-1}$, the rate of excitation delivery to PSII centers far exceeded the capacity of
236 photosynthetic electron transport between PSII and PSI. This resulted in a progressive saturation
237 of the observed fluorescence transients within the first 40-60 flashlets, with a rate proportional to
238 the functional absorption cross section at particular wavelength. The saturation phase was
239 followed by 90 flashlets applied at exponentially-increasing time interval starting at 20 μs , over a
240 period of 250 ms. As the average excitation power decreased, the fluorescence signal relaxed
241 with a kinetics mostly defined by the rates of electron transport between PSII and PSI. Each
242 sample measurement consisted of an average of 32 transients, and each sample was measured
243 three times at each wavelength. Blanks were obtained by gently filtering sample water through a
244 0.2 μm syringe filter and processing it in the same manner as the samples. Recorded fluorescence
245 transients were processed with FRRF software (<http://soliense.com/>) to estimate photosystem II
246 maximum *in vivo* fluorescence (F_m), maximum photochemical efficiency (F_v/F_m), the
247 functional absorption cross section (σ_{PSII}) for all Chl *a*-containing cells (excitation wavelength of
248 470 nm) and phycoerythrin-containing plankton (e.g. *Synechococcus*, excitation wavelength of
249 505 nm), and the kinetics of the PSII-PSI electron transport.

250

251 *Flow cytometry*

252 Samples (2 mL of seawater) for subsequent flow cytometric enumeration of picoplankton
253 were immediately fixed with glutaraldehyde (0.25% v/v final concentration) upon collection,
254 kept at room temperature in the dark for 15 min, then flash frozen and kept at -80°C until
255 processing. Abundances of *Prochlorococcus*, *Synechococcus*, photosynthetic picoeukaryotes
256 (PPEs), and heterotrophs were enumerated using a BD Biosciences Influx Cell Sorter (BD
257 Biosciences, San Jose, CA, USA) equipped with a 488 nm Sapphire laser (Coherent, Santa Clara,
258 CA, USA) using a 70 µm nozzle. All fixed seawater samples were pre-filtered using
259 a CellTrics® filter with 30 µm mesh (Partec, Swedesboro, NJ, USA). *Synechococcus*
260 populations were identified based on the presence of phycoerythrin (orange fluorescence; 572–
261 27 photomultiplier tube, PMT) and all other non-phycoerythrin populations were identified using
262 forward scatter (FSC) as a proxy for cell size and Chl *a* content (red fluorescence; 692–20 PMT).
263 To enumerate non-pigmented cells (heterotrophs), samples were stained with SYBR® Green I
264 nucleic acid stain (Lonza Inc., Allendale, NJ, USA) according to the protocol described in Marie
265 et al. 1999. To determine the abundances of non-pigmented heterotrophs with High Nucleic Acid
266 content (HNA cells), the abundance of *Prochlorococcus* and *Synechococcus* cells were
267 subtracted from all HNA cells. Data collection was triggered in the forward scatter (FSC)
268 channel for photosynthetic cells and in the green channel (531-40 PMT) for SYBR-stained cells.
269 Photosynthetic cells were counted for 10 min; SYBR-positive cells were counted for 1.5 min.
270 Cell counts were processed in FlowJo v10.0.7 (Tree Star, Inc., Ashland, OR, USA).

271

272 *DNA extraction*

273 1-2 L of seawater from each incubation bottle was filtered onto 0.2 µm Supor membrane
274 filters (Pall Corp., Ann Arbor, MI, USA) using peristaltic pumps. The filters were placed in

275 sterile 2.0 mL microcentrifuge tubes containing 0.5 and 1 mm diameter glass beads (Biospec,
276 Bartlesville, OK, USA), flash frozen in liquid N₂, and stored at -80°C until DNA extraction.
277 DNA was extracted using the Qiagen DNeasy Plant kit (Valencia, CA, USA), with modifications
278 outlined in Moisander et al. (2008) to improve recovery of high quality DNA. The final wash
279 steps and DNA elution were automated using a QIAcube robotic workstation (Qiagen). DNA
280 quantity and quality was measured using a NanoDrop (Thermo Scientific, Waltham, MA, USA)
281 with an average DNA yield 1100±900 ng L⁻¹ seawater.

282

283 *16S rRNA gene sequencing and sequence read processing*

284 Community composition was analyzed based on sequences of the V3-V4 hypervariable
285 region of the 16S rRNA gene using universal primers targeting Bacteria, Bakt_341F and
286 Bakt_805R (Herlemann et al. 2011). Primers were modified with common sequence linkers
287 (Moonsamy et al. 2013) to facilitate library preparation. PCR amplifications were carried out in
288 triplicate 25 µL reactions for each sample, with the following reaction conditions: 1X Platinum
289 Taq PCR buffer –Mg (Invitrogen, Carlsbad, CA), 2.5 mM MgCl₂, 200 µM dNTP mix, 0.25 µM
290 of both forward and reverse primers, 3 U Platinum Taq DNA Polymerase (Invitrogen), and 1 uL
291 of the DNA template. DNA was amplified using the following thermocycling conditions: initial
292 denaturation at 95°C for 5 min, 25 cycles of denaturation at 95°C for 40 s, annealing at 53°C for
293 40 s, elongation at 72°C for 60 s, and a final elongation at 72°C for 7 min. Pooled amplicons
294 underwent 10 more amplification cycles to add sequencing adaptors and sample-specific
295 barcodes at the DNA Services Facility at the University of Illinois, Chicago, using the targeted
296 amplicons sequencing approach described in Green et al. (2015). After the second round of PCR
297 amplification performed by DNA Services at UIC, library concentrations were equalized using

298 SequelPrep purification plates (ThermoFisher Scientific). Paired-end reads were sequenced at the
299 W.M. Keck Center for Comparative and Functional Genomics at the University of Illinois at
300 Urbana-Champaign using Illumina MiSeq technology. Sequences of the 16S rRNA gene
301 amplicons were obtained from a total of 91 samples that included samples in three replicates
302 from T0, T24 and T48 for both experiments. There were on average 9986 reads per sample
303 (median=9990, minimum=9664, and maximum=10340 reads per sample). De-multiplexed raw
304 paired-end reads were merged using PEAR (Zhang et al. 2014). Assembled sequences were then
305 quality filtered (split_libraries_fasta.py; phred score of 20) and chimeras were removed using a
306 de novo approach (identify_chimeric_seqs.py) in QIIME (Caporaso et al. 2010). Operational
307 taxonomic units (OTU) were defined at 99% nucleotide similarity using the usearch6.1
308 clustering method (Edgar 2010; pick_otus.py) and representative sequences were retrieved
309 (pick_rep_set.py) in QIIME. The taxonomy of representative sequences was assigned using a
310 Greengenes reference database (http://greengenes.secondgenome.com/downloads/database/13_5;
311 DeSantis et al. 2006), and the assign_taxonomy.py QIIME script. We used the default
312 parameters for the uclust consensus taxonomy assigner through QIIME (the minimum percent
313 similarity for a taxonomic assignment was 0.9). The 16S rRNA gene sequences were deposited
314 in Sequence Read Archive at National Center for Biotechnology Information (NCBI,
315 <http://www.ncbi.nlm.nih.gov/sra>) under BioProject accession number PRJNA358607.

316

317 *Oligotyping*

318 The oligotyping approach separates individual taxa, ‘oligotypes’, within closely related
319 organisms based on high entropy nucleotide positions in the 16S rRNA gene sequence (Eren et
320 al. 2013). In order to define oligotypes for *Prochlorococcus* and *Synechococcus*, we used the

321 oligotyping pipeline version 2.0 (May 27, 2015) and followed the instructions available at
322 <http://oligotyping.org> (Eren et al. 2013). The oligotyping analysis was performed separately for
323 both *Prochlorococcus* and *Synechococcus*. A total of 395,666 and 10,271 reads were obtained
324 for *Prochlorococcus* and *Synechococcus*, respectively, from samples taken at T0 and T48 in the
325 two experiments. Before the oligotyping analysis, the sequences were aligned using PyNAST
326 (Caporaso et al. 2010) and Greengenes 16S rRNA gene reference database (gg_13_5 version
327 available at <http://greengenes.secondgenome.com/>). Shannon entropy calculations were followed
328 by the oligotyping analysis, which was run until each oligotype had converged (as described in
329 Eren et al. 2013). The following parameters were chosen for both *Prochlorococcus* and
330 *Synechococcus* oligotyping analyses: $a=0.1$ and $s=2$, where ‘a’ is the minimum percent
331 abundance of an oligotype in at least one sample and ‘s’ is the minimum number of samples
332 where an oligotype is expected to be present (Eren et al. 2013). The minimum substantial
333 abundance criterion, M, determines the minimum abundance of the most abundant unique
334 sequence in an oligotype and helps to reduce noise (Eren et al. 2013). For *Prochlorococcus* and
335 *Synechococcus* oligotyping analyses, M was 100 and 20, respectively. To assign taxonomy, the
336 representative sequences of the oligotypes were searched against the reference genome database
337 at NCBI using blastn version 2.3.0+ (Altschul et al. 1990). The BLAST search was done with the
338 default parameters, and all best hits were saved. Because some strains within the genera
339 *Prochlorococcus* and *Synechococcus* have identical 16S rRNA V3-V4 region sequences, a
340 representative sequence of an oligotype often was equally identical to several strains. We called
341 a group of such identical strains an eStrain, and the strains within each eStrain are reported in
342 Table S1. Note that the sequences belonging to one oligotype are identical at the selected
343 nucleotide positions within the amplified ~441 nt region, but may vary at other positions within

344 the 16S rRNA gene. Next, the relative abundance of oligotypes was used to calculate the
345 absolute abundance using the cell counts for *Prochlorococcus* and *Synechococcus*, and the
346 absolute numbers were used in further analyses.

347

348 *Shifts in community composition*

349 The changes in composition of the heterotrophic microbial communities and
350 *Prochlorococcus* and *Synechococcus* communities, were analyzed using the *Phyloseq* package
351 (McMurdie and Holmes 2013) within R (The R Core Team 2013, <http://www.r-project.org>). For
352 heterotrophic community analysis, phylum “Cyanobacteria” (that includes sequences from
353 chloroplasts) were excluded, and the selected taxa were required to have a minimum of 50 reads
354 total, resulting in 676090 sequences total in all samples (minimum of 6195, median of 7040, and
355 maximum of 9493 sequences per sample). Ecological distances among the samples were
356 estimated with the Bray-Curtis and Jaccard indices. To compare the community shifts, resulting
357 from different treatments, Principal Coordinate Analysis (PCoA) was applied on the distance
358 matrices. In addition, the relative read abundances for heterotrophic microbial communities were
359 standardized to the median sequence depths (rarefied). There was little difference in the depth of
360 sequencing among the samples (maximum difference <600 reads with a mean of ~10K reads per
361 sample) and the PCoA results for standardized data were similar to the results from the non-
362 standardized data.

363

364 *Software*

365 All statistical analyses were done in R (The R Core Team 2013, [http://www.r-](http://www.r-project.org)
366 [project.org](http://www.r-project.org)): two-sample t-test for comparisons of means for Chl *a*, PP, abundances, and FRRF

367 measurements between treatments and controls and between treatments. To test for the observed
368 differences in community composition among treatments, analysis of similarities was done on
369 the Bray-Curtis dissimilarity distance matrix (*anosim* function within the “vegan” package in R,
370 Oksanen et al. 2016). The statistic R in analysis of similarities is based on the difference of mean
371 ranks between the groups and within groups, ranges from -1 to 1, and R value of 0 indicates
372 random groupings. In addition to analysis of similarities, analysis of variance (*adonis* function in
373 “vegan”) was done on the Bray-Curtis dissimilarity matrix. Data were visualized using the
374 ggplot2 package (Wickham 2009) in R, and all final figures were prepared for publication using
375 Adobe Illustrator.

376

377 **Results**

378 *Initial conditions*

379 The physical and chemical conditions at the two experimental sites differed substantially. TZ
380 (Station 38) was located in the transition zone between the California Current and the NPSG
381 along the eastern margin of an anticyclonic eddy (Figs. 1a&b). GY (Station 52) was located in
382 the oligotrophic waters of the central gyre and further west in the NPSG in an area of relatively
383 low eddy activity (Fig. 1b). Both salinity and seawater temperature were higher at GY than at TZ
384 (Table 1). The mixed layer depth was twice as deep at GY (48 m) in comparison to TZ (24 m)
385 (Fig. 1c).

386 Concentrations of $\text{NO}_3^- + \text{NO}_2^-$ in near-surface waters were low ($<3 \text{ nmol L}^{-1}$) at both
387 experimental sites (Table 1) while concentrations of NH_4^+ were higher at TZ ($58 \pm 3 \text{ nmol L}^{-1}$ vs.
388 $36 \pm 10 \text{ nmol L}^{-1}$ at GY). Soluble reactive phosphorus (SRP) concentrations were approximately
389 three-fold higher and concentrations of Si(OH)_4 were 1.5-fold higher at TZ compared to GY.

390 Finally, surface concentrations of dissolved Fe were below detection (LOD=0.058 nmol L⁻¹) at
391 both sites.

392 The abundance of total picoplankton cells was approximately equal at the two
393 experimental stations (Table 1, 4.7±0.8 x 10⁵ and 5.0±0.6 x 10⁵ cells mL⁻¹ at GY and TZ,
394 respectively) but the composition of the communities was somewhat different. Phytoplankton
395 cells were 1.5-fold more abundant at GY relative to TZ (Table 1) mainly due to
396 *Prochlorococcus*; however, the difference was not significant (1.6±0.5 x 10⁵ cells mL⁻¹ and
397 1.0±0.5 x 10⁵ cells mL⁻¹ at GY and TZ, respectively). *Synechococcus* was approximately 100-
398 times less abundant than *Prochlorococcus* at both sites (1.2±0.8 x 10³ and 3.9±0.7 x 10³ cells
399 mL⁻¹ at GY and TZ, respectively). *Synechococcus* abundance was 3-times higher at TZ
400 compared to GY, accounting for 0.8% and 0.2% of total cells at each site, respectively.
401 Likewise, the abundance of photosynthetic picoeukaryotes (PPE) was low at both sites
402 (1.14±0.03 x 10³ and 2.5±0.2 x 10³ cells mL⁻¹ at GY and TZ, respectively), with TZ having ~2.3-
403 times more PPE cells than GY. PPE accounted for ≤0.5% of the total cell population at either
404 site. Finally, heterotrophic bacteria were enumerated as either high nucleic acid (HNA)- or low
405 nucleic acid (LNA)-containing populations, the latter of which was more abundant (Table 1).
406 The abundances of each HNA and LNA cells were similar between the two sites (1.2±0.2 x 10⁵
407 and 2.5±0.3 x 10⁵ for HNA and LNA cells, respectively).

408 Despite the differences in physicochemical conditions and the composition of the microbial
409 communities, the initial concentrations of Chl *a* and rates of PP were similar at the two stations
410 (Table 1). In contrast, maximum photochemical efficiency of PSII measured at excitation
411 wavelength of 470 nm (F_v/F_{m470}) was higher at TZ (0.51±0.01) than at GY (0.34±0.02), while

412 no significant difference was detected between stations with respect to functional absorption
413 cross-section of PSII ($\sigma_{\text{PSII-470}}$).

414

415 *Phytoplankton Chl a concentrations and PP rates*

416 All tested N forms and Fe alone resulted in significant increases in Chl *a* concentrations
417 and rates of PP after 48 hrs of incubation at both locations, and the response at GY was in
418 general larger than at TZ (Fig. 2). Additional nutrients (for example through the addition of Fe or
419 filtered deep water, FDW) did not enhance the response observed for the N forms further.

420 The largest increases in concentrations of Chl *a* at TZ after 48 hrs of incubation were
421 observed in response to urea and NH_4^+ additions ($0.19 \pm 0.01 \mu\text{g L}^{-1}$), >3.5-times higher in
422 comparison to the Control (no nutrient addition, Chl_{cnt} , $0.052 \pm 0.002 \mu\text{g L}^{-1}$) (Fig. 2a). Addition
423 of NO_3^- produced a 1.4-times increase in Chl *a* over Chl_{cnt} at TZ. At GY, the urea addition
424 resulted in the largest responses in Chl *a* concentration ($0.18 \pm 0.01 \mu\text{g L}^{-1}$) compared to the Chl_{cnt}
425 ($0.034 \pm 0.003 \mu\text{g L}^{-1}$), followed by the NH_4^+ and NO_3^- additions (3-times higher relative to
426 Chl_{cnt}).

427 Changes in PP were similar to the Chl *a* responses in both experiments, with 4-times
428 higher carbon fixation rates observed in response to additions of urea and NH_4^+ at TZ (1.40 ± 0.07
429 $\mu\text{mol C L}^{-1} \text{d}^{-1}$) and 8-times higher rates in response to urea at GY ($1.3 \pm 0.1 \mu\text{mol C L}^{-1} \text{d}^{-1}$) in
430 comparison to the Controls at 48 hours (PP_{cnt} ; Fig. 2b). The NO_3^- addition at TZ resulted in 2.5-
431 times higher PP rates relative to the PP_{cnt} . Both NH_4^+ and NO_3^- yielded >5-times higher PP
432 relative to the PP_{cnt} after 48 hrs of incubation at GY.

433 In addition to stimulation by N substrates, the Fe addition alone produced a significant
434 increase in Chl *a* concentrations (40% increase over Chl_{cnt}) and rates of PP (>20% increase over

435 PP_{cnt}) at both locations after 48 hours of incubation (Fig. 2 and Table S2). However, the
436 additions of NO₃⁻ + Fe (N+Fe) and FDW stimulated Chl *a* concentrations and PP rates to the
437 same degree as the NO₃⁻ addition alone at both station (Fig. 2, Table S2).

438

439 *Photophysiology*

440 Use of FRRF to interrogate phytoplankton photophysiological responses (Fm, Fv/Fm and
441 σ_{PSII}) to nutrient amendments demonstrated that the phytoplankton community at both sites was
442 affected by the addition of the individual N compounds, and the response was stronger and more
443 variable at GY than at TZ (Fig. 3). Addition of Fe alone also had a stimulating effect on the
444 photosystem activity; however, N+Fe did not have an additional stimulating effect compared to
445 NO₃⁻ alone.

446 Fm at 470 nm (Fm₄₇₀; inclusive of all Chl-containing plankton) increased significantly
447 after 24 hrs of incubation in response to all N substrates in both experiments (Fig. 3). At TZ, all
448 N sources resulted in a similar increase in Fm₄₇₀ relative to the Control by 48 hrs. At GY, urea,
449 NH₄⁺ and N+Fe all resulted in large increases in Fm₄₇₀ (300%) compared with the Control by 48
450 hrs, while the increase in the NO₃⁻ and FDW treatments was slightly less (200%). Finally, Fe
451 addition yielded a lower but significant (Table S3) increase in Fm₄₇₀ (50% relative to the
452 Control) by 48 hrs at both locations.

453 The addition of the various N substrates also stimulated phycoerythrin-containing
454 phytoplankton (Fm₅₀₅), but the response to different N forms at the two locations varied (Fig 3).
455 Fm₅₀₅ was significantly stimulated in the NO₃⁻ and NH₄⁺ treatments by 24 hrs at both stations
456 while Fm₅₀₅ increased in response to urea only at TZ. By 48 hrs at TZ, NH₄⁺, NO₃⁻, N+Fe and
457 FDW additions all increased the Fm₅₀₅ response (>130%) relative to the Control (Fig. 3b). At

458 GY, additions of NH_4^+ and N+Fe resulted in a larger Fm_{505} response (>300% increase relative to
459 the Control; Fig. 3b), while the responses to urea, NO_3^- and FDW were slightly less (>200%
460 increase relative to the Control). Fe had a significant but weak effect on Fm_{505} by 48 hrs at both
461 stations (Fig. 3b, Table S3).

462 Fv/Fm was significantly influenced by all N forms and by Fe largely at GY. The initial
463 Fv/Fm₄₇₀ was higher at the TZ station (0.51 ± 0.01 and 0.34 ± 0.02 at TZ and GY, respectively). At
464 GY, all N additions resulted in a significant increase in Fv/Fm₄₇₀ in comparison to the Control by
465 24 hrs, with the highest (145%) increase in response to NO_3^- and NH_4^+ (Fig. 3c). At TZ, only the
466 NO_3^- addition resulted in a significant increase in Fv/Fm₄₇₀ and only after 48 hrs (Fig. 3c and
467 Table S3). Similar to Fv/Fm₄₇₀, the initial Fv/Fm₅₀₅ at GY (0.41 ± 0.03) was lower than at TZ
468 (0.50 ± 0.02). At GY, all N and Fe additions resulted in an increase in Fv/Fm₅₀₅ similar to that of
469 Fv/Fm₄₇₀ (Fig. 3d). However, in contrast to responses in Fv/Fm₄₇₀, Fv/Fm₅₀₅ was weakly affected
470 by the three N forms by 24 hrs at TZ.

471 The response observed for σ_{PSII} to the additions of urea and NH_4^+ was anti-correlated
472 with the responses observed for Chl *a* concentrations and PP. σ_{PSII} observed at 470 nm
473 significantly decreased at TZ in response to the addition of both urea and NH_4^+ relative to the
474 Control (Fig. 3e); in contrast, σ_{PSII} decreased only in response to urea at the GY station.
475 Likewise, a significant decrease in response to urea was also observed for σ_{PSII} at 505 nm but
476 only at GY (Fig. 3f, Table S3). A weak stimulating effect (<30% of the Control) on σ_{PSII} was
477 observed for phytoplankton with 505 nm excitation wavelength in response to N+Fe and FDW
478 additions at GY and in response to N+Fe and NH_4^+ at TZ (Fig. 3e&f, Table S3).

479

480 *Response of the phytoplankton and bacterial groups*

481 Phytoplankton and non-photosynthetic bacteria had different qualitative and quantitative
482 responses to N and Fe substrates, with variations depending on location.

483 All N forms resulted in increases in *Prochlorococcus* abundance at TZ and GY (Fig. 4a).
484 The largest response at TZ was observed in the NH_4^+ and urea treatments ($2.2 \pm 0.3 \times 10^5$ cells mL^{-1}), where *Prochlorococcus* abundance was 4-times higher than in the Control after 48 hrs. In the
485 NO_3^- , N+Fe, and FDW treatments, *Prochlorococcus* abundance was 2-times higher than in the
486 Control. At GY, urea produced the largest increase in *Prochlorococcus* abundance by 48 hrs
487 ($2.8 \pm 0.1 \times 10^5$ cells mL^{-1} , 3-times higher than the Control) followed by NO_3^- with 2-times higher
488 *Prochlorococcus* abundance compared to the Control. The effects of NH_4^+ , N+Fe, and FDW on
489 *Prochlorococcus* abundances were less (~50% increase over the Control) at GY. Fe stimulated
490 *Prochlorococcus* abundance at TZ (~40% increase over the Control) but not at GY.

492 *Synechococcus* abundance also increased significantly in response to the addition of urea,
493 NO_3^- , N+Fe, and Fe at both stations, and the response to N was greatest at GY (Fig. 4b).
494 *Synechococcus* abundances following the urea or NO_3^- additions were 3.5 ± 0.5 and $3.2 \pm 0.3 \times 10^3$
495 cells mL^{-1} (>1.3-times higher than in the Controls) at TZ and GY, respectively. Addition of
496 NH_4^+ resulted in a decrease in *Synechococcus* abundance at TZ and only a small increase at GY;
497 however, the effect was not significantly different from the Control by 48 hrs at either station
498 (Table S4). *Synechococcus* abundance at both locations responded to Fe additions. While not
499 significantly different from the effect of N at TZ, the Fe effect was significantly lower than the
500 effects of urea and NO_3^- at GY (Table S4). Notably, addition of N+Fe resulted in a significantly
501 higher *Synechococcus* response in comparison to Fe alone at both stations (Fig. 4b, Table S4).

502 PPE abundance increased significantly in response to all N forms and to Fe at both
503 stations. Overall larger increases in PPE abundance were observed at GY (Fig. 4c) than at TZ.

504 NO_3^- resulted in a high degree of variability between the replicates at TZ, which contributed to a
505 lower statistical significance ($t_{(2)}=2.4$, $p=0.06$). PPE abundances in response to all N at TZ were
506 ~ 1.5 -times higher than in the Control and were similar for all nutrients including Fe (average
507 PPE abundance in all N and Fe additions was $\sim 2.1 \pm 0.4 \times 10^3$ cells mL^{-1}). At GY by 48 hours,
508 additions of NH_4^+ , urea, NO_3^- , N+Fe, and FDW resulted in $>100\%$ increases in PPE abundance
509 relative to the Control and Fe-alone treatment (average $\sim 1.1 \pm 0.2 \times 10^3$ cells mL^{-1} in the N
510 additions; Fig. 4c).

511 HNA abundance responded to additions of NH_4^+ , NO_3^- , and N+Fe at both stations (up to
512 125% increase over the Control by 48 hrs, Fig. 4d). At GY, the HNA cells also increased 1.5-
513 times the Control in response to the FDW addition. The increase in HNA abundance at GY, but
514 not at TZ, was significant by 24 hrs (Table S4). In contrast to the HNA cells, only the N+Fe
515 addition at TZ station resulted in a significant increase (38% relative to the Control) in the
516 abundance of LNA cells by 48 hrs (Fig. 4e). No significant increase in the LNA cell abundance
517 was observed at GY (Fig. 4e, Table S4).

518

519 *Shift in microbial community composition*

520 To further evaluate the effect of N on the microbial communities at these two sites, and to
521 assess whether differences in microbial community composition accompanied the observed
522 changes in PP, Chl a , FRRF, and cell abundance, we amplified and sequenced the V3-V4
523 hypervariable region of the 16S rRNA gene. Based on the 16S rRNA gene relative abundances,
524 the initial microbial community composition (Control T0) at the genus level was similar at both
525 locations and was dominated by Cyanobacteria (genus *Prochlorococcus*, 31-34% of total 16S
526 rRNA gene sequences) and *Alphaproteobacteria* (family *Pelagibacteraceae*, 30-33% of total

527 16S rRNA gene sequences), followed by other *Alphaproteobacteria* (no taxonomic assignment,
528 7-8% of total 16S rRNA gene sequences), *Gammaproteobacteria* (*Halomonadaceae*: *C. Portiera*,
529 5-7% of total 16S rRNA gene sequences), and *Actinobacteria* (*Acidimicrobiales*: OCS155, 2-3%
530 of total 16S rRNA gene sequences) (Fig. 5a). *Synechococcus* was a minor component of the
531 microbial community at both locations (0.7% of total 16S rRNA sequences). Relative
532 abundances of chloroplast 16S rRNA sequences varied between the two locations. At TZ,
533 abundances of *Haptophyceae* and *Stramenopiles* each were 1.9% of total 16S rRNA gene
534 sequences. At GY, relative abundances of *Haptophyceae* and *Stramenopiles* in the initial
535 community were 1.1% and 0.8%, respectively.

536 A shift in microbial community composition at the genus level in response to all N
537 additions was detected within 48 hrs in both experiments with the strongest response to NH_4^+
538 (Fig. 5). Both Jaccard and Bray-Curtis ecological indices produced similar results (Fig. 5b and
539 S1a). Differences in the Bray-Curtis dissimilarities between treatments were significant
540 (difference of mean ranks between the groups $R > 0.77$, $p < 0.001$ in both experiments). At both
541 locations, the response to all N forms was characterized by the increase in relative abundance of
542 representatives from the Gammaproteobacteria families *Alteromonadaceae* and
543 *Oceanospirillaceae* (Fig. 5a). At TZ, the relative abundance of *Alteromonadaceae* (unassigned
544 genus) increased from 0.2% in the Control to 41%, 55% and 57% of all reads in the urea, NH_4^+ ,
545 and NO_3^- additions at T48, respectively. At GY, the relative abundance of *Alteromonadaceae*
546 (unassigned genus) increased from 0.3% in the Control to 15%, 34% and 36% of all reads in the
547 urea, NO_3^- , and NH_4^+ additions at T48, respectively. Relative abundance of *Oleispira* (family
548 *Oceanospirillaceae*) increased significantly in the N additions, but only at GY: from 0.1% in the
549 Control to 9%, 10% and 20% of all reads in NH_4^+ , urea, and NO_3^- additions at T48, respectively.

550 The relative abundance of another *Oceanospirillaceae* genus (*Oleibacter*) increased from
551 undetectable in the Control to as much as 5% of all reads in the N additions at TZ. Addition of
552 NH_4^+ resulted in the most distinct microbial community, with the shift observed within 24 hrs at
553 both stations (Fig. 5a&b). Relative abundance of 16S rRNA gene sequences from representatives
554 of the genus *Phaeobacter* (Alphaproteobacteria: *Rhodobacteraceae*) were associated with the
555 NH_4^+ additions and increased from undetectable in the Control to 5% and 19% of all reads in the
556 NH_4^+ addition in both GY and TZ at T48, respectively (Fig. S1c). Addition of urea resulted in a
557 less pronounced change in microbial community composition, especially at TZ. Finally, Fe
558 addition did not significantly influence community composition at both locations.

559 The shift in microbial community composition in response to all N forms at GY was
560 faster than at TZ and detected by 24 hrs after the addition of nutrients (Figs. 5a&b). Samples
561 taken 24 hrs after the start of the incubation experiment at TZ were most similar to the Controls
562 and T0 samples. In contrast, T48 samples from treatments with any N addition at TZ clustered
563 separately from the T0 and T24 samples, Controls, and Fe addition treatment. At GY, all of the
564 N addition treatments clustered separately from the Controls, T0, and Fe addition within 24 hrs.

565

566 *Response of picocyanobacteria to N*

567 Given the great genetic diversity within marine microbial genera (e.g. Kashtan et al.
568 2014), we examined changes in abundance of individual taxa within *Prochlorococcus* and
569 *Synechococcus* populations at high resolution by using an oligotyping approach (Eren et al.
570 2013). The responses to different N forms and Fe varied between and within *Prochlorococcus*
571 and *Synechococcus* genera.

572 *Prochlorococcus* populations differed between the two locations (Fig. 6a). A total of 31
573 oligotypes were identified in *Prochlorococcus* communities across both experiments based on 7
574 nucleotide positions with high entropy (as described in the Methods). The *Prochlorococcus*
575 communities at TZ and GY were dominated by strains from the High Light I (HLI) and High
576 Light II (HLII) clades, respectively. The oligotypes MED4-oligo1 (100% identical to
577 *Prochlorococcus* MED4, HLI) and MIT9515-oligo1 (100% identical to *Prochlorococcus*
578 MIT9515, HLI) were on average 74% and 10%, respectively, of all of the *Prochlorococcus*
579 sequences in the Control T0 sample at TZ (Table 2). At GY, these oligotypes comprised 1% of
580 total *Prochlorococcus* sequences in the Control T0 (Table 2). The most abundant oligotype at
581 GY, MIT9301-oligo1 (100% identical to *Prochlorococcus* MIT9301, HLII, and strains with
582 similar sequence of the 16S rRNA gene region, Table S1), comprised on average 66% of the
583 *Prochlorococcus* sequences. The next most abundant, the MIT9312-oligo1 oligotype (100%
584 identical to *Prochlorococcus* MIT9312, HLII, and related strains, Table S1), was on average
585 22% of the *Prochlorococcus* sequences at GY station. Both of the most abundant oligotypes at
586 GY were <1% of the sequences in the Control T0 from TZ (Table 2). Representatives of the Low
587 Light I (LLI) clade were present at both locations, although only as minor portions of the
588 community (Table 2).

589 The addition of different N forms had differential effects on the *Prochlorococcus*
590 populations in both experiments by 48 hrs (Figs. 6b-d). While urea addition resulted in a
591 consistent increase in abundance of all *Prochlorococcus* oligotypes and clades, NH_4^+ and NO_3^-
592 resulted in variable responses within the *Prochlorococcus* communities and between the two
593 locations. Differences in the Bray-Curtis dissimilarities for *Prochlorococcus* communities
594 between treatments were higher than within treatments (analysis of similarities for TZ: $R=0.36$,

595 p=0.007, and GY: R=0.51, p=0.002, see Methods). The Bray-Curtis dissimilarity index showed
596 that urea and NH_4^+ additions resulted in a shift in the *Prochlorococcus* community composition
597 that was most distinct from the effects of the rest of the treatments and Controls at TZ, while the
598 urea and NO_3^- additions resulted in the strongest shift in comparison to the effects of the rest of
599 the treatments (and Controls) at GY (Fig. 6b). These patterns paralleled the general response of
600 total *Prochlorococcus* abundance (measured by flow cytometry) and were observed for the most
601 abundant *Prochlorococcus* oligotypes in each experiment (Fig. 6c&d). However, the minor
602 oligotype NATL1A-oligo1 (LLI) had a larger response to urea and NO_3^- than to NH_4^+ at TZ (Fig.
603 6d). At GY, some members of HLII, HLI and LLI clades had no significant responses to NH_4^+
604 (Fig. 6c and S2).

605 Some *Prochlorococcus* oligotypes had different responses to nutrient amendments
606 between the two sites. For example, the two dominant oligotypes at TZ, MED4-oligo1 and
607 MIT9515-oligo1, had the greatest response to urea and NH_4^+ (Fig. 6d). However, although they
608 were minor (<1%) components of the *Prochlorococcus* community at GY, these oligotypes had
609 the greatest responses to urea and NO_3^- (Fig. 6c and S2). The responses by *Prochlorococcus*
610 PAC1-oligo1 (LLI) also varied between the two sites (Fig. 6d and S2).

611 Similar to *Prochlorococcus*, *Synechococcus* communities at the two locations were
612 distinct; however, the most dominant *Synechococcus* oligotypes were the same at the two
613 locations (Fig. 7a). A total of 11 oligotypes were distinguished for *Synechococcus* based on 11
614 nucleotide positions with high entropy. *Synechococcus* oligotypes derived from both clades II
615 and IV were most abundant at TZ, whereas *Synechococcus* oligotypes from clade II were most
616 abundant at GY. *Synechococcus* oligotype CC9605-oligo1, with 100% identity to *Synechococcus*
617 CC9605 (clade II), was the most abundant at both locations, constituting on average of 35% and

618 61% of *Synechococcus* 16S rRNA gene sequences at TZ and GY, respectively (Table 2).
619 Another oligotype from clade II, CC9605-oligo2, was also present at both stations (Table 2).
620 Two oligotypes derived from clade IV (CC9902-oligo1 and CC9902-oligo2 with 100% and
621 99.7% identity, respectively, to *Synechococcus* CC9902) contributed 39% to the *Synechococcus*
622 community at TZ. The least abundant oligotypes present at both stations included representatives
623 from clade V (Table 2).

624 N additions had a larger effect on *Synechococcus* community composition at GY than at
625 TZ (Fig. 7b). Differences in the Bray-Curtis dissimilarities for *Synechococcus* communities
626 between treatments were significantly higher than within treatments at GY (analysis of
627 similarities for GY: $R=0.54$, $p=0.001$ compared to TZ: $R=0.19$, $p=0.07$). The Bray-Curtis
628 dissimilarity index showed a weak separation of samples with NO_3^- , urea, N+Fe, and FDW
629 additions from the Controls and samples with NH_4^+ and Fe additions at TZ. At GY, all nutrients,
630 including Fe, resulted in a strong shift in the *Synechococcus* community, with the urea addition
631 resulting in the most distinct responses compared to other nutrient additions.

632 Similar to *Prochlorococcus*, N forms had a differential effect on *Synechococcus*
633 oligotypes, resulting in distinct *Synechococcus* populations by 48 hr (Figs. 7c&d). The response
634 of oligotypes also varied between the sites. Consistent with the response in total *Synechococcus*
635 abundance, the dominant oligotype CC9902-oligo1 (clade IV) responded to NO_3^- , urea, Fe, and
636 FDW at TZ. In contrast, the oligotype CC9605-oligo5 (clade II) had a weak increase in
637 abundance in response to urea availability relative to the Control at TZ (Fig. 7d). However, all N
638 forms and Fe affected this oligotype abundance at GY (Fig. 7c), with the largest effect seen in
639 the NO_3^- and N+Fe additions. Urea had the largest effect on the less abundant oligotype CC9605-
640 oligo2 (clade II) at GY. Moreover, less abundant oligotypes had distinct responses compared to

641 the responses of the dominant oligotypes. For example, oligotype KORDI100-oligo1 (Clade V)
642 had a significant increase in cell abundance only in response to N+Fe at TZ (Fig. 7d).

643

644 **Discussion**

645 The effect of N availability on biological processes in the ocean is one of the most
646 studied topics in marine microbiology; however, we still know little about the complex
647 interactions between the diverse microbial communities and different N compounds used by
648 specific microorganisms. We investigated the effects of NO_3^- , NH_4^+ , and urea as sources of N on
649 microbial community activity (PP and photosynthetic efficiency), and community composition
650 (based on major microbial group cell counts and 16S rRNA gene sequence) in the open ocean
651 waters of the North Pacific Ocean. All N forms tested had significant effects on microbial
652 communities at the investigated sites in the NPSG within 48 hrs (Table 3). Limitation of PP and
653 maximum photochemical efficiency of PSII by N has been reported in other low-latitude
654 oligotrophic waters, such as in the North Atlantic Ocean (Graziano et al. 1996; Moore et al.
655 2006, 2008; Davey et al. 2008). Moreover, N was the major limiting nutrient constraining total
656 phytoplankton biomass in the Western South Pacific Ocean (Moisander et al. 2012) and in the
657 South Pacific Gyre (Van Wambeke et al. 2008). In addition to N, either P or Fe can co-limit
658 picoplankton cell growth in the North Atlantic (Davey et al. 2008). While the effect of SRP was
659 not specifically tested in our study, the addition of FDW (which had elevated SRP and NO_3^-
660 concentrations, Table 1) resulted in similar responses as the addition of N alone, suggesting that
661 P did not co-limit plankton biomass or productivity during our experiments.

662

663 *Stimulating effect of urea on phytoplankton*

664 The importance of urea as an N source for phytoplankton was demonstrated decades ago
665 (McCarthy et al. 1972b; Price and Harrison 1988; Antia et al. 1991; Fan et al. 2003). The urease
666 gene has been found in a variety of marine microorganisms, including the cyanobacteria
667 *Synechococcus* and *Prochlorococcus*, eukaryotic phytoplankton (haptophytes, diatoms,
668 prasinophytes), and heterotrophic bacteria (*Roseobacteraceae*, *Pelagibacter*,
669 Gammaproteobacteria HTCC2207) (Baker et al. 2009; Collier et al. 2009; Solomon et al. 2010).
670 Urea concentrations in the surface open oceans appear highly variable in space and time, ranging
671 from 0.3 to 0.7 $\mu\text{mol N L}^{-1}$ (Bronk et al. 2002; Painter et al. 2008). In the current study, urea was
672 added at much higher concentrations (2.5 and 5.0 $\mu\text{mol of N L}^{-1}$) than previously reported in situ
673 concentrations; however, our results demonstrated that all major groups of phytoplankton
674 responded to the urea additions, with responses differing between the two locations examined
675 (Table 3). Previous studies have also described variable responses in rates of uptake and growth
676 in phytoplankton when urea was supplied as the sole N source (Cochlan and Harrison 1991;
677 Lomas and Glibert 2000; Moore et al. 2002; Fan et al. 2003; Solomon et al. 2010).

678 Our results suggest that urea may be an important N source for *Prochlorococcus* (Figs.
679 6&7), which is responsible for a large fraction of PP in the open oceans (Vaulot et al. 1995;
680 Campbell et al. 1997; DuRand et al. 2001). *Prochlorococcus* clades HLI and HLII dominated at
681 the TZ and GY stations, respectively, consistent with the observations that these clades occupy
682 different niches, with the shift from the HLI to the HLII clade reported at the threshold of $\sim 23^{\circ}\text{C}$
683 in summer (Farrant et al. 2016; Larkin et al. 2016). *Prochlorococcus* HLI and HLII are the most
684 abundant *Prochlorococcus* clades (Johnson et al. 2006) and the majority of sequenced
685 *Prochlorococcus* genomes have urea utilization and transporter genes (Kettler et al. 2007;
686 Scanlan et al. 2009). The results of our study showed that both clades responded significantly to

687 urea additions, demonstrating large increases in abundances, >300% relative to the Controls.
688 The oligotyping analysis of *Prochlorococcus* 16S rRNA gene sequences further showed that
689 *Prochlorococcus* community composition was strongly influenced by urea additions at both
690 sites. The high transcription of the urea transporter gene in natural populations of
691 *Prochlorococcus* found in metatranscriptomic studies (Frias-Lopez et al. 2008; Gifford et al.
692 2011; Shi et al. 2011) suggests that *Prochlorococcus* actively acquire urea. Indeed, rates of urea
693 uptake by *Prochlorococcus* in the Sargasso Sea were found to be similar or faster than NH_4^+
694 uptake rates (Casey et al. 2007), and a significant relationship was observed between
695 *Prochlorococcus* abundances and bulk urea uptake rates in the Northern Atlantic Ocean (Painter
696 et al. 2008). While utilization of urea by picocyanobacteria has been shown before (Rippka et al.
697 2000; Moore et al. 2002), our study suggests that urea may be an important source of N
698 supporting the growth of natural populations of *Prochlorococcus*.

699

700 *Variable responses of phytoplankton to NH_4^+ and NO_3^-*

701 In contrast to urea, the effects of NO_3^- and NH_4^+ on phytoplankton communities varied
702 between the sites. The addition of NH_4^+ significantly stimulated rates of PP both at the TZ and
703 GY stations. At GY, both NO_3^- and NH_4^+ additions resulted in the similar degree of enhancement
704 in PP, but responses to these additions had a less stimulating effect than that of urea. The PP
705 response pattern at TZ was paralleled by changes in *Prochlorococcus* cell abundance and
706 community composition. The different responses to the two N forms were likely the result of
707 uptake preferences by different phytoplankton groups for NO_3^- and NH_4^+ , as well as different
708 degrees of Fe limitation experienced among the phytoplankton groups at TZ (discussed below).

709 Genetic and physiological differences may help explain the differential responses of
710 *Prochlorococcus* populations to NH_4^+ and NO_3^- between the two experimental sites. Genes
711 encoding pathways for $\text{NO}_3^-/\text{NO}_2^-$ assimilation have been found in some *Prochlorococcus* HL
712 and LL strains, and these strains are able to grow solely on NO_3^- as an N source (Martiny et al.
713 2009; Berube et al. 2015). Thus, not surprisingly, naturally-occurring *Prochlorococcus*
714 populations from HLI, HLII, and LLI clades responded to NO_3^- additions at low NH_4^+
715 concentrations at both stations in our study. Laboratory studies indicate that *Prochlorococcus*
716 growth on NO_3^- is slower than growth on NH_4^+ (Berube et al. 2015) and such results could
717 explain the differences in cell abundances in response to NO_3^- and NH_4^+ additions at TZ.
718 Additionally, the genome of *Prochlorococcus* MIT9515 (HLI), a strain that was abundant at TZ,
719 has two copies of the *amt* gene which encodes an NH_4^+ transporter (Scanlan et al. 2009) and this
720 strain may be more competitive for NH_4^+ than the strains that were present at GY station. In
721 contrast, the genome of *Prochlorococcus* MIT0604 (HLII, with the V3-V4 region of the 16S
722 rRNA gene sequence 100% identical to *Prochlorococcus* MIT9301, the eStrain that was
723 dominant at GY) has two clusters of NO_3^- assimilation genes (Berube et al. 2015). Finally,
724 another HLII strain (SB strain) present at GY has the most extensive gene suite for N utilization,
725 including NO_3^- , urea, and cyanate assimilation genes (Berube et al. 2015). In addition to the
726 genetic and physiological differences, microbial interactions likely influenced the observed
727 changes in abundance. For example, it is possible that NO_3^- additions may have stimulated
728 growth of mixotrophic eukaryotes that consumed *Prochlorococcus* cells (Hartmann et al. 2013).
729 In general, the N-limitation of *Prochlorococcus* cell abundance observed in the present study
730 contrasted with results observed in the Western South Pacific Ocean where *Prochlorococcus*

731 HLII responded to Fe and P (Moisander et al. 2012), a finding that may reflect lower N:Fe or
732 N:P supply ratios in the northern hemisphere (Ward et al. 2013).

733 It was surprising that *Synechococcus* abundance showed little response to the NH_4^+
734 addition. NH_4^+ is thought to be the preferred N substrate by cyanobacteria over NO_3^- because of
735 the higher energetic cost for reduction and assimilation of NO_3^- . However, culture studies
736 showed that under sub-saturating irradiance, growth rates of marine *Synechococcus* on NO_3^-
737 were similar to growth rates on NH_4^+ (Collier et al. 2012). Considering that *Prochlorococcus* and
738 heterotrophic bacteria were orders of magnitude more abundant than *Synechococcus* at both
739 stations, and that *Synechococcus* cells have a lower surface area to volume ratio than
740 *Prochlorococcus* (Morel et al. 1993), *Synechococcus* may have been at a competitive
741 disadvantage for NH_4^+ uptake. However, the fact that ~50% of the added NH_4^+ remained after 48
742 hrs of incubation (Table S5) suggests that *Synechococcus* preferred NO_3^- as an N source,
743 although the mechanism for N substrate preference remains unclear (Collier et al. 2012).

744 In contrast to *Synechococcus*, the photosynthetic picoeukaryotes showed the greatest
745 increase in abundance in the NH_4^+ addition, but only at GY. The lack of a PPE response to NH_4^+
746 at TZ may be related to Fe availability (see below). A preference for NH_4^+ over NO_3^- and urea
747 has been previously shown for PPEs in culture, such as the prasinophyte *Micromonas* (Cochlan
748 and Harrison 1991). Interestingly, the prasinophytes *Micromonas* and *Ostreococcus* have genes
749 for two types of the NH_4^+ transporters (AMT), one of which is similar to bacterial *amt* (Derelle et
750 al. 2006; McDonald et al. 2010). Transcription of this AMT gene is up-regulated in response to
751 N-depletion (McDonald et al. 2010). Likewise, transcription of the NH_4^+ transporter genes in
752 response to N-depletion has also been shown for diatoms (Allen et al. 2005; Bowler et al. 2008).
753 The data presented here supports the observations of previous studies that eukaryotic

754 phytoplankton can successfully compete for NH_4^+ with smaller bacterial cells (Bradley et al.
755 2010).

756

757 *Fe limitation of phytoplankton growth and activity in the CCS*

758 Fe availability affected the abundance of all groups of phytoplankton and rates of PP at
759 TZ. Fe limitation of phytoplankton growth in the CCS is believed to be due to the rapid depletion
760 of Fe relative to NO_3^- in the upwelled waters that travel offshore as filaments (Bruland et al.
761 2001; Biller and Bruland 2013). In addition, the TZ site was in an anticyclonic eddy containing
762 open ocean water with relatively high SRP, but otherwise low nutrient and Chl *a* concentrations.
763 The mixing of open ocean water at the sampling site is further supported by the mixture of
764 coastal and open ocean phytoplankton communities found at this site. For example, the coastal
765 *Synechococcus* clade IV, usually prevalent in colder nutrient-rich waters, was present at the same
766 abundance as *Synechococcus* clade II, which is the dominant open ocean clade (Sohm et al.
767 2016). The high abundance of *Prochlorococcus* at this site also indicated an input of oligotrophic
768 gyre waters. Thus, the mixing of the oligotrophic gyre waters at TZ may have contributed to the
769 low Fe availability.

770 The genetic differences between the communities at the two stations is likely an
771 additional factor contributing to the stronger response to Fe at TZ. For example, coastal strains of
772 phytoplankton are adapted to have higher cellular Fe quotas than open ocean strains (Brand
773 1991; Sunda et al. 1991; Strzepek and Harrison 2004). Moreover, *Prochlorococcus* MED4
774 (HLI), which was abundant at TZ, has been shown to be especially sensitive to Fe availability
775 (Thompson et al. 2011). Finally, *Prochlorococcus* has a larger number of genes for coping with
776 low Fe environments than *Synechococcus* (Rocap et al. 2003; Scanlan et al. 2009), which may

777 explain why *Prochlorococcus* had a greater response to N than to Fe additions, in contrast to
778 *Synechococcus* at TZ. Thus, a combination of factors, genetic and environmental, may have
779 resulted in the strong community response to Fe at TZ. These results provide further support for
780 Fe limitation of phytoplankton growth in the CCS transition zone.

781 Furthermore, some microbial populations were most likely N and Fe co-limited at TZ. An
782 independent type of co-limitation of biomass (Arrigo 2005; Saito et al. 2008) may explain why
783 the addition of N and Fe together did not enhance the response in Chl *a* and primary productivity
784 relative to N or Fe additions alone. If only a small fraction of the community are N and Fe co-
785 limited in comparison to the N-limited fraction, then the effect of N+Fe may not be significant in
786 bulk measurements. The responses by the *Synechococcus* oligotypes support this hypothesis: The
787 oligotype identical to *Synechococcus* KORDI-100 (clade V) had greater relative abundances in
788 N+Fe in comparison to the Fe or N additions alone. However, this oligotype comprised only 5%
789 of the total *Synechococcus* population, and thus did not contribute significantly to the responses
790 in total *Synechococcus* biomass. The two other *Synechococcus* oligotypes at TZ (originating
791 from clades II and IV) showed similar responses to N+Fe, Fe, or NO₃⁻. These were the most
792 abundant *Synechococcus* oligotypes at TZ and likely comprised many sub-populations that could
793 not be distinguished at the 16S rRNA gene resolution. Thus, using the high resolution
794 oligotyping approach allowed us to distinguish the diversity of responses within microbial
795 populations, such as to nutrient co-limitation, which were not reflected in the bulk
796 measurements.

797

798 *Responses of heterotrophic microbial communities to N substrates*

799 The heterotrophic community responded to N forms differently than the phototrophic
800 community. The NH_4^+ followed by the NO_3^- additions at both locations resulted in the strongest
801 shifts in heterotrophic community composition, as estimated from 16S rRNA gene relative
802 abundances (Table 3). Additionally, HNA cell abundances increased in the NO_3^- and NH_4^+
803 additions at both sites regardless of the phytoplankton response (Table 3). The shift was largely
804 due to the increase in the relative abundance of Gammaproteobacteria (*Oceanospirillaceae*,
805 *Alteromonadaceae*, and *Vibrionaceae*) and Alphaproteobacteria (*Phaeobacter*), the copiotrophic
806 microbial taxa known to respond rapidly to enrichments of surface seawater with nutrients or
807 associated with phytoplankton blooms (González et al. 2000; Shi et al. 2012; Beier et al. 2014;
808 El-Swais et al. 2015; Sosa et al. 2015). Smaller in size than some phytoplankton cells in general,
809 heterotrophic bacteria may have a competitive advantage by taking up available NH_4^+ and NO_3^-
810 rapidly, thereby actively competing for macronutrients, as has been reported in many other
811 studies (Eppley et al. 1977; Wheeler and Kirchman 1986; Kirchman 1994; Mills et al. 2008;
812 Bradley et al. 2010).

813

814 *Differences between the TZ and GY stations*

815 The greatest differences in microbial community responses to N additions between the
816 two locations were in the timing and degree of the responses. The shift in heterotrophic microbial
817 community composition at GY was observed earlier than at TZ. This may be due to the distinct
818 phototrophic communities at each location. For example, *Prochlorococcus* HLI and
819 *Synechococcus* Clades II and IV were dominant at TZ, and *Prochlorococcus* HLII and
820 *Synechococcus* Clade II were dominant at GY. However, our study suggests that the microbial
821 community was under more severe nutrient limitation at GY than at TZ. The nutricline at GY

822 was deeper than at TZ, and the microbes at GY had likely been nutrient limited longer than those
823 at the TZ station. The low initial Fv/Fm of the phototrophic community at GY and the significant
824 and rapid (in 24 hrs) increase in Fv/Fm upon N additions suggest that new N contributed to the
825 building of new photosynthetic proteins and that photosynthetic activity at GY was strongly N-
826 limited (Suggett et al. 2009). The increase in PP following N additions was also significantly
827 greater at GY than at TZ. As previously shown in cultures, N pre-conditioning affects how fast
828 phytoplankton respond to N (Conway et al. 1976; Price and Harrison 1988). Additionally,
829 phytoplankton species have the ability to change substrate affinities and uptake potentials
830 depending on the degree of nutrient limitation (Conway and Harrison 1977). Thus, microbial
831 community composition and N pre-conditioning may determine the timing and degree of the
832 responses to N substrates in the North Pacific.

833

834 **Conclusions**

835 N substrates have differential effects on different phytoplankton groups, and the degree
836 and rapidity of the responses depend on the pre-existing physicochemical conditions (e.g. Price
837 and Harrison 1988). Our study extends previous findings by using a combination of techniques
838 to measure total microbial community physiological and functional responses as well as shifts in
839 microbial community composition and changes in abundance of phytoplankton populations at
840 high taxonomic resolution. The results of our study indicate that N availability limited PP and
841 accumulation of microbial biomass during our sampling in the open ocean waters of the North
842 Pacific. Moreover, we observed distinct differences in rates of PP, accumulation of biomass, and
843 community composition in response to additions of urea, NH_4^+ , and NO_3^- . The growth of some
844 populations of phytoplankton, especially *Synechococcus* and PPE, was also limited by Fe in the

845 CCS region. Our results also suggest the heterotrophic microbial community successfully
846 competed for inorganic N sources at both experimental sites. Finally, besides the differences in
847 community composition, the pre-existing conditions at each site likely influenced the timing and
848 degree of the responses to N perturbations by both phytoplankton and heterotrophic community.

849 There is strong evidence that future oceans will experience changes in temperature and N
850 supply (Kim et al. 2014). The genetics of populations determines how environmental factors
851 affect their ecologies and evolution (e.g. Larkin et al. 2016), and the results of our study imply
852 that changes in N substrate availability favors different components of the phytoplankton
853 community in different oceanic regions. More importantly, because phytoplankton taxa vary in
854 elemental stoichiometry (Sterner and Elser 2002; Bertilsson et al 2003; Heldal et al. 2003),
855 physiology (e.g. Moore et al. 2002), viral resistance (Stoddart et al. 2007) and DOM production
856 (Becker et al. 2014), changes in phytoplankton community composition would impact
857 biogeochemical cycles, as well as ecological processes. The results of our study underline the
858 importance to better understand the complex interactions between diverse microbial populations
859 and nutrient availability in the oceans.

860

861 **Acknowledgements**

862 We thank the captain, crew and technicians of the R/V *New Horizon* for assistance and support
863 during the research cruise. We thank Mary Hogan (UCSC) for helping in preparations for the
864 cruises and DNA extraction, Joaquin Pampin Baro (GEOMAR) for providing support for the
865 trace-metal free work, Dr. Stefan Green and his staff at the DNA Services Facility (the
866 University of Illinois, Chicago) for next generation sequencing consultation, Ed Boring (UCSC)
867 for bioinformatics assistance. In addition, Susan Curless, Brenner Wai, Alexa Nelson, and Stu

868 Goldberg all provided laboratory support of this project. This work was supported by awards
869 from the National Science Foundation Dimensions in Biodiversity program (1241221), Center
870 for Microbial Oceanography: Research and Education (NSF EF0424599), and the Deutsche
871 Forschungsgemeinschaft as part of Sonderforschungsbereich 754: 'Climate-Biogeochemistry
872 Interactions in the Tropical Ocean' (to EPA).
873

874 **References**

- 875 Allen, A. E. 2005. Beyond sequence homology: Redundant ammonium transporters in a marine
 876 diatom are not functionally equivalent. *J. Phycol.* **41**: 4-6.
- 877 Allen, A. E., M. G. Booth, M. E. Frischer, P. G. Verity, J. P. Zehr, and S. Zani. 2001. Diversity
 878 and detection of nitrate assimilation genes in marine bacteria. *Appl. Environ. Microbiol.*
 879 **67**: 5343-5348.
- 880 Allen, A. E., A. Vardi, and C. Bowler. 2006. An ecological and evolutionary context for
 881 integrated nitrogen metabolism and related signaling pathways in marine diatoms. *Curr.*
 882 *Opin. Plant Biol.* **9**: 264-273.
- 883 Altschul, S. F., W. Gish, W. Miller, E. W. Myers, and D. J. Lipman. 1990. Basic local alignment
 884 search tool. *J. Mol. Biol.* **215**: 403-410.
- 885 Aluwihare, L. I., and T. Meador. 2008. Chemical composition of marine dissolved organic
 886 nitrogen, p. 95-140. In D. G. Capone, D. A. Bronk, M. R. Mulholland and E. J. Carpenter
 887 [eds.], *Nitrogen in the Marine Environment*, 2nd ed. Elsevier Academic Press Inc.
- 888 Antia, N. J., P. J. Harrison, and L. Oliveira. 1991. The role of dissolved organic nitrogen in
 889 phytoplankton nutrition, cell biology and ecology. *Phycologia* **30**: 1-89.
- 890 Arrigo, K. R. 2005. Marine microorganisms and global nutrient cycles. *Nature* **437**: 349-355.
- 891 Baker, K. M., C. J. Gobler, and J. L. Collier. 2009. Urease gene sequences from algae and
 892 heterotrophic bacteria in axenic and nonaxenic phytoplankton cultures. *J. Phycol.* **45**:
 893 625-634.
- 894 Becker, J. W., and others. 2014. Closely related phytoplankton species produce similar suites of
 895 dissolved organic matter. *Front. Microbiol.* **5**: 14.
- 896 Beier, S., A. R. Rivers, and M. A. Moran, I. Obernosterer. 2015. The transcriptional response of
 897 prokaryotes to phytoplankton-derived dissolved organic matter in seawater. *Environ.*
 898 *Microbiol.* **17**: 3466–3480.
- 899 Bertilsson, S., O. Berglund, D. M. Karl, and S. W. Chisholm. 2003. Elemental composition of
 900 marine *Prochlorococcus* and *Synechococcus*: Implications for the ecological
 901 stoichiometry of the sea. *Limnol. Oceanogr.* **48**: 1721-1731.
- 902 Berube, P. M., and others. 2015. Physiology and evolution of nitrate acquisition in
 903 *Prochlorococcus*. *ISME J.* **9**: 1195-1207.
- 904 Bidigare, R. R. 1983. Nitrogen excretion by marine zooplankton, p. 385-409. In E. J. Carpenter
 905 and D. G. Capone [eds.], *Nitrogen in the marine environment*. Academic Press.
- 906 Biller, D. V., and K. W. Bruland. 2013. Sources and distributions of Mn, Fe, Co, Ni, Cu, Zn, and
 907 Cd relative to macronutrients along the central California coast during the spring and
 908 summer upwelling season. *Mar. Chem.* **155**: 50-70.
- 909 Biller, D. V., and K. W. Bruland. 2014. The central California Current transition zone: A broad
 910 region exhibiting evidence for iron limitation. *Prog. Oceanogr.* **120**: 370-382.
- 911 Bonnet, S., and others. 2008. Nutrient limitation of primary productivity in the Southeast Pacific
 912 (BIOSOPE cruise). *Biogeosciences* **5**: 215-225.
- 913 Böttjer, D., J.E. Dore, D.M. Karl, R.M. Letelier, C. Mahaffey, S.T. Wilson, and M.J. Church.
 914 2016. Temporal variability in nitrogen fixation and particulate nitrogen export at Station
 915 ALOHA. *Limnol. Oceanogr.* doi: 10.1002/lno.10386.
- 916 Bowler, C., and others. 2008. The *Phaeodactylum* genome reveals the evolutionary history of
 917 diatom genomes. *Nature* **456**: 239-244.

- 918 Bradley, P. B., and others. 2010. Inorganic and organic nitrogen uptake by phytoplankton and
919 heterotrophic bacteria in the stratified Mid-Atlantic Bight. *Estuarine Coastal Shelf Sci.*
920 **88**: 429-441.
- 921 Brand, L. E. 1991. Minimum iron requirements of marine-phytoplankton and the implications for
922 the biogeochemical control of new production. *Limnol. Oceanogr.* **36**: 1756-1771.
- 923 Bronk, D. A. 2002. Dynamics of DON, p 153–247. In: D. A. Hansell and C. A. Carlson [eds.],
924 *Biogeochemistry of marine dissolved organic matter*. Academic Press.
- 925 Bronk, D. A., P. M. Glibert, T. C. Malone, S. Banahan, and E. Sahlsten. 1998. Inorganic and
926 organic nitrogen cycling in Chesapeake Bay: autotrophic versus heterotrophic processes
927 and relationships to carbon flux. *Aquat. Microb. Ecol.* **15**: 177-189.
- 928 Bruland, K. W., E. L. Rue, and G. J. Smith. 2001. Iron and macronutrients in California coastal
929 upwelling regimes: Implications for diatom blooms. *Limnol. Oceanogr.* **46**: 1661-1674.
- 930 Campbell, L., H. B. Liu, H. A. Nolla, and D. Vaultot. 1997. Annual variability of phytoplankton
931 and bacteria in the subtropical North Pacific Ocean at Station ALOHA during the 1991-
932 1994 ENSO event. *Deep-Sea Res., Part I.* **44**: 167-192.
- 933 Caporaso, J. G., and others. 2010. QIIME allows analysis of high-throughput community
934 sequencing data. *Nat. Methods.* **7**: 335-336.
- 935 Capotondi, A., M. A. Alexander, N. A. Bond, E. N. Curchitser, and J. D. Scott. 2012. Enhanced
936 upper ocean stratification with climate change in the CMIP3 models. *J. Geophys. Res.:*
937 *Oceans* **117**: C04031.
- 938 Casey, J. R., M. W. Lomas, J. Mandrecki, and D. E. Walker. 2007. *Prochlorococcus* contributes
939 to new production in the Sargasso Sea deep chlorophyll maximum. *Geophys. Res. Lett.*
940 **34**: L10604.
- 941 Chisholm, S. W., R. J. Olson, E. R. Zettler, R. Goericke, J. B. Waterbury, and N. A.
942 Welschmeyer. 1988. A novel free-living prochlorophyte abundant in the oceanic euphotic
943 zone. *Nature* **334**: 340-343.
- 944 Cochlan, W. P., and P. J. Harrison. 1991. Uptake of nitrate, ammonium, and urea by nitrogen-
945 starved cultures of *Micromonas-pusilla* (*Prasinophyceae*) - transient responses. *J. Phycol.*
946 **27**: 673-679.
- 947 Collier, J. L., K. M. Baker, and S. L. Bell. 2009. Diversity of urea-degrading microorganisms in
948 open-ocean and estuarine planktonic communities. *Environ. Microbiol.* **11**: 3118-3131.
- 949 Collier, J. L., R. Lovindeer, Y. Xi, J. C. Radway, and R. A. Armstrong. 2012. Differences in
950 growth and physiology of marine *Synechococcus* (Cyanobacteria) on nitrate versus
951 ammonium are not determined solely by nitrogen source redox state. *J. Phycol.* **48**: 106-
952 116.
- 953 Conway, H. L., and P. J. Harrison. 1977. Marine diatoms grown in chemostats under silicate or
954 ammonium limitation. 4. Transient-response of *Chaetoceros-debilis*, *Skeletonema-*
955 *costatum*, and *Thalassiosira-gravida* to a single addition of limiting nutrient. *Mar. Biol.*
956 **43**: 33-43.
- 957 Conway, H. L., P. J. Harrison, and C. O. Davis. 1976. Marine diatoms grown in chemostats
958 under silicate or ammonium limitation. 2. Transient-response of *Skeletonema-costatum* to
959 a single addition of limiting nutrient. *Mar. Biol.* **35**: 187-199.
- 960 Corner, E. D. S., and B. S. Newell. 1967. On nutrition and metabolism of zooplankton. 4. Forms
961 of nitrogen excreted by *Calanus*. *J. Mar. Biol. Assoc. U. K.* **47**: 113-120.
- 962 Davey, M., G. A. Tarran, M. M. Mills, C. Ridame, R. J. Geider, and J. LaRoche. 2008. Nutrient
963 limitation of picophytoplankton photosynthesis and growth in the tropical North Atlantic.

- 964 *Limnol. Oceanogr.* **53**: 1722-1733.
- 965 Derelle, E., and others. 2006. Genome analysis of the smallest free-living eukaryote
966 *Ostreococcus tauri* unveils many unique features. *Proc. Natl. Acad. Sci. U. S. A.* **103**:
967 11647-11652.
- 968 DeSantis, T. Z., and others. 2006. Greengenes, a chimera-checked 16S rRNA gene database and
969 workbench compatible with ARB. *Appl. Environ. Microbiol.* **72**: 5069-5072.
- 970 Dore, J. E., T. Houlihan, D. V. Hebel, G. Tien, L. Tupas, and D. M. Karl. 1996. Freezing as a
971 method of sample preservation for the analysis of dissolved inorganic nutrients in
972 seawater. *Mar. Chem.* **53**: 173-185.
- 973 Dore, J. E., and D. M. Karl. 1996. Nitrification in the euphotic zone as a source for nitrite,
974 nitrate, and nitrous oxide at Station ALOHA. *Limnol. Oceanogr.* **41**: 1619-1628.
- 975 Duce, R. A., and others. 2008. Impacts of atmospheric anthropogenic nitrogen on the open
976 ocean. *Science* **320**: 893-897.
- 977 Dugdale, R. C., and J. J. Goering. 1967. Uptake of new and regenerated forms of nitrogen in
978 primary productivity. *Limnol. Oceanogr.* **12**: 196-206.
- 979 DuRand, M. D., R. J. Olson, and S. W. Chisholm. 2001. Phytoplankton population dynamics at
980 the Bermuda Atlantic Time-series station in the Sargasso Sea. *Deep-Sea Res., Part II.* **48**:
981 1983-2003.
- 982 Edgar, R. C. 2010. Search and clustering orders of magnitude faster than BLAST. *Bioinformatics*
983 **26**: 2460-2461.
- 984 El-Swais, H., K. A. Dunn, J. P. Bielawski, W. K. W. Li, and D. A. Walsh. 2015. Seasonal
985 assemblages and short-lived blooms incoastal north-west Atlantic Ocean
986 bacterioplankton. *Environ. Microbiol.* **17**: 3642-3661.
- 987 Eppley, R. W., and B. J. Peterson. 1979. Particulate organic-matter flux and planktonic new
988 production in the deep ocean. *Nature* **282**: 677-680.
- 989 Eppley, R. W., J. H. Sharp, E. H. Renger, M. J. Perry, and W. G. Harrison. 1977. Nitrogen
990 assimilation by phytoplankton and other microorganisms in surface waters of central
991 North Pacific Ocean. *Mar. Biol.* **39**: 111-120.
- 992 Eren, A. M., and others. 2013. Oligotyping: differentiating between closely related microbial
993 taxa using 16S rRNA gene data. *Meth. Ecol. Evol.* **4**: 1111-1119.
- 994 Fan, C., P. M. Glibert, J. Alexander, and M. W. Lomas. 2003. Characterization of urease activity
995 in three marine phytoplankton species, *Aureococcus anophagefferens*, *Prorocentrum*
996 *minimum*, and *Thalassiosira weissflogii*. *Mar. Biol.* **142**: 949-958.
- 997 Farrant, G. K., and others. 2016. Delineating ecologically significant taxonomic units from
998 global patterns of marine picocyanobacteria. *Proc. Natl. Acad. Sci. U. S. A.* **113**: E3365-
999 E3374.
- 1000 Fawcett, S. E., M. Lomas, J. R. Casey, B. B. Ward, and D. M. Sigman. 2011. Assimilation of
1001 upwelled nitrate by small eukaryotes in the Sargasso Sea. *Nat. Geosci.* **4**: 717-722.
- 1002 Frias-Lopez, J., and others. 2008. Microbial community gene expression in ocean surface waters.
1003 *Proc. Natl. Acad. Sci. U. S. A.* **105**: 3805-3810.
- 1004 Garside, C. 1982. A chemi-luminescent technique for the determination of nanomolar
1005 concentrations of nitrate and nitrite in sea-water. *Mar. Chem.* **11**: 159-167.
- 1006 Gifford, S. M., S. Sharma, J. M. Rinta-Kanto, and M. A. Moran. 2011. Quantitative analysis of a
1007 deeply sequenced marine microbial metatranscriptome. *ISME J.* **5**: 461-472.
- 1008 González, J. M., R. Simó, R. Massana, J. S. Covert, E. O. Casamayor, C. Pedrós-Alió, and M. A.
1009 Moran. 2000. Bacterial community structure associated with a

1010 dimethylsulfoniopropionate-producing North Atlantic algal bloom. *Appl. Environ.*
1011 *Microbiol.* **66**: 4237-4246.

1012 Graziano, L. M., R. J. Geider, W. K. W. Li, and M. Olaizola. 1996. Nitrogen limitation of North
1013 Atlantic phytoplankton: Analysis of physiological condition in nutrient enrichment
1014 experiments. *Aquat. Microb. Ecol.* **11**: 53-64.

1015 Green, S. J., R. Venkatramanan, and A. Naqib. 2015. Deconstructing the Polymerase Chain
1016 Reaction: understanding and correcting bias associated with primer degeneracies and
1017 primer-template mismatches. *PLoS One* **10**: 21.

1018 Gruber, N., and J. N. Galloway. 2008. An Earth-system perspective of the global nitrogen cycle.
1019 *Nature* **451**: 293-296.

1020 Hallam, S. J., and others. 2006. Pathways of carbon assimilation and ammonia oxidation
1021 suggested by environmental genomic analyses of marine *Crenarchaeota*. *PLoS Biol.* **4**:
1022 520-536.

1023 Hansell, D. A., and J. J. Goering. 1989. A method for estimating uptake and production-rates for
1024 urea in seawater using [¹⁴C] urea and [¹⁵N] urea. *Can. J. Fish. Aquat. Sci.* **46**: 198-202.

1025 Hartmann, M., M. V. Zubkov, D. J. Scanlan, and C. Lepere. 2013. In situ interactions between
1026 photosynthetic picoeukaryotes and bacterioplankton in the Atlantic Ocean: evidence for
1027 mixotrophy. *Environ. Microbiol. Rep.* **5**: 835-840.

1028 Haldal, M., D. J. Scanlan, S. Norland, F. Thingstad, and N. H. Mann. 2003. Elemental
1029 composition of single cells of various strains of marine *Prochlorococcus* and
1030 *Synechococcus* using X-ray microanalysis. *Limnol. Oceanogr.* **48**: 1732-1743.

1031 Herlemann, D. P. R., M. Labrenz, K. Jurgens, S. Bertilsson, J. J. Waniek, and A. F. Andersson.
1032 2011. Transitions in bacterial communities along the 2000 km salinity gradient of the
1033 Baltic Sea. *ISME J.* **5**: 1571-1579.

1034 Johnson, Z. I., E. R. Zinser, A. Coe, N. P. McNulty, E. M. S. Woodward, and S. W. Chisholm.
1035 2006. Niche partitioning among *Prochlorococcus* ecotypes along ocean-scale
1036 environmental gradients. *Science* **311**: 1737-1740.

1037 Karner, M. B., E. F. DeLong, and D. M. Karl. 2001. Archaeal dominance in the mesopelagic
1038 zone of the Pacific Ocean. *Nature* **409**: 507-510.

1039 Kettler, G. C., and others. 2007. Patterns and implications of gene gain and loss in the evolution
1040 of *Prochlorococcus*. *PLoS Genet.* **3**: 2515-2528.

1041 Kim, I. N., and others. 2014. Increasing anthropogenic nitrogen in the North Pacific Ocean.
1042 *Science* **346**: 1102-1106.

1043 Kirchman, D. L. 1994. The uptake of inorganic nutrients by heterotrophic bacteria. *Microbiol.*
1044 *Ecol.* **28**: 255-271.

1045 Kolber, Z. S., O. Prasil, and P. G. Falkowski. 1998. Measurements of variable chlorophyll
1046 fluorescence using fast repetition rate techniques: defining methodology and
1047 experimental protocols. *Biochim. Biophys. Acta, Bioenerg.* **1367**: 88-106.

1048 Larkin, A. A., and others. 2016. Niche partitioning and biogeography of high light adapted
1049 *Prochlorococcus* across taxonomic ranks in the North Pacific. *ISME J.* **10**: 1555-1567.

1050 Li, Q. P., J. Z. Zhang, F. J. Millero, and D. A. Hansell. 2005. Continuous colorimetric
1051 determination of trace ammonium in seawater with a long-path liquid waveguide
1052 capillary cell. *Mar. Chem.* **96**: 73-85.

1053 Lomas, M. W., and P. M. Glibert. 2000. Comparisons of nitrate uptake, storage, and reduction in
1054 marine diatoms and flagellates. *J. Phycol.* **36**: 903-913.

1055 Marie, D., F Partensky, D. Vaultot, and C. Brussaard. 1999. Enumeration of phytoplankton,

1056 bacteria, and viruses in marine samples, p. 11.11.1-11.11.15. In J. P. Robinson [ed],
1057 *Current protocols in cytometry*. John Wiley and Sons, Inc.

1058 Martiny, A. C., S. Kathuria, and P. M. Berube. 2009. Widespread metabolic potential for nitrite
1059 and nitrate assimilation among *Prochlorococcus* ecotypes. *Proc. Natl. Acad. Sci. U. S. A.*
1060 **106**: 10787-10792.

1061 Mayzaud, P. 1973. Respiration and nitrogen excretion of zooplankton. 2. Studies of metabolic
1062 characteristics of starved animals. *Mar. Biol.* **21**: 19-28.

1063 McCarthy, J. J. 1972a. Uptake of urea by marine phytoplankton. *J. Phycol.* **8**: 216-222.
1064 ---. 1972b. Uptake of urea by natural populations of marine phytoplankton. *Limnol. Oceanogr.*
1065 **17**: 738-748.

1066 McCarthy, J. J., and R. W. Eppley. 1972. Comparison of chemical, isotopic, and enzymatic
1067 methods for measuring nitrogen assimilation of marine phytoplankton. *Limnol.*
1068 *Oceanogr.* **17**: 371-382.

1069 McDonald, S. M., J. N. Plant, and A. Z. Worden. 2010. The mixed lineage nature of nitrogen
1070 transport and assimilation in marine eukaryotic phytoplankton: a case study of
1071 *Micromonas*. *Mol. Biol. Evol.* **27**: 2268-2283.

1072 McMurdie, P. J., and S. Holmes. 2013. phyloseq: An R package for reproducible interactive
1073 analysis and graphics of microbiome census data. *PLoS One* **8**: 11.

1074 Mills, M. M., and others. 2008. Nitrogen and phosphorus co-limitation of bacterial productivity
1075 and growth in the oligotrophic subtropical North Atlantic. *Limnol. Oceanogr.* **53**: 824-
1076 834.

1077 Mills, M. M., C. Ridame, M. Davey, J. La Roche, and R. J. Geider. 2004. Iron and phosphorus
1078 co-limit nitrogen fixation in the eastern tropical North Atlantic. *Nature* **429**: 292-294.

1079 Mitamura, O., and Y. Saijo. 1981. Studies on the seasonal-changes of dissolved organic-carbon,
1080 nitrogen, phosphorus and urea concentrations in lake Biwa. *Arch. Hydrobiol.* **91**: 1-14.

1081 Moisander, P. H., R. A. Beinart, M. Voss, and J. P. Zehr. 2008. Diversity and abundance of
1082 diazotrophic microorganisms in the South China Sea during intermonsoon. *ISME J.* **2**:
1083 954-967.

1084 Moisander, P. H., R. F. Zhang, E. A. Boyle, I. Hewson, J. P. Montoya, and J. P. Zehr. 2012.
1085 Analogous nutrient limitations in unicellular diazotrophs and *Prochlorococcus* in the
1086 South Pacific Ocean. *ISME J.* **6**: 733-744.

1087 Montoya, J. P., E. J. Carpenter, and D. G. Capone. 2002. Nitrogen fixation and nitrogen isotope
1088 abundances in zooplankton of the oligotrophic North Atlantic. *Limnol. Oceanogr.* **47**:
1089 1617-1628.

1090 Moonsamy, P. V., and others. 2013. High throughput HLA genotyping using 454 sequencing and
1091 the Fluidigm Access Array (TM) system for simplified amplicon library preparation.
1092 *Tissue Antigens* **81**: 141-149.

1093 Moore, C. M., and others. 2013. Processes and patterns of oceanic nutrient limitation. *Nat.*
1094 *Geosci.* **6**: 701-710.

1095 Moore, C. M., and others. 2008. Relative influence of nitrogen and phosphorus availability on
1096 phytoplankton physiology and productivity in the oligotrophic sub-tropical North
1097 Atlantic Ocean. *Limnol. Oceanogr.* **53**: 291-305.

1098 Moore, L. R., A. F. Post, G. Rocap, and S. W. Chisholm. 2002. Utilization of different nitrogen
1099 sources by the marine cyanobacteria *Prochlorococcus* and *Synechococcus*. *Limnol.*
1100 *Oceanogr.* **47**: 989-996.

1101 Morel, A., Y. H. Ahn, F. Partensky, D. Vaultot, and H. Claustre. 1993. *Prochlorococcus* and

1102 *Synechococcus* - a comparative-study of their optical-properties in relation to their size
1103 and pigmentation. *J. Mar. Res.* **51**: 617-649.

1104 Morris, R. M., and others. 2002. SAR11 clade dominates ocean surface bacterioplankton
1105 communities. *Nature* **420**: 806-810.

1106 Mulholland, M. R., and M. W. Lomas. 2008. Nitrogen uptake and assimilation, p. 303-384. In D.
1107 G. Capone, D. A. Bronk, M. R. Mulholland and E. J. Carpenter [eds.], *Nitrogen in the*
1108 *Marine Environment*, 2nd Edition. Elsevier Academic Press Inc.

1109 Obata, H., H. Karatani, and E. Nakayama. 1993. Automated-determination of iron in seawater by
1110 chelating resin concentration and chemiluminescence detection. *Anal. Chem.* **65**: 1524-
1111 1528.

1112 Oksanen, J., and others. 2016. vegan: Community Ecology Package. R package version 2.4-1.
1113 <https://CRAN.R-project.org/package=vegan>.

1114 Ortega-Retuerta, E., W. H. Jeffrey, J. F. Ghiglione, and F. Joux. 2012. Evidence of heterotrophic
1115 prokaryotic activity limitation by nitrogen in the Western Arctic Ocean during summer.
1116 *Polar Biol.* **35**: 785-794.

1117 Price, N. M., and P. J. Harrison. 1988. Urea uptake by Sargasso Sea phytoplankton - saturated
1118 and in situ uptake rates. *Deep-Sea Res., Part II.* **35**: 1579-1593.

1119 Quay, P. D., C. Peacock, K. Björkman, and D. M. Karl. 2010. Measuring primary production
1120 rates in the ocean: Enigmatic results between incubation and non-incubation methods at
1121 Station ALOHA. *Glob. Biogeochem. Cycles* **24**: GB3014. doi:10.1029/2009GB003665.

1122 Rippka, R., and others. 2000. *Prochlorococcus marinus* Chisholm et al. 1992 subsp pastoris
1123 subsp nov strain PCC 9511, the first axenic chlorophyll a(2)/b(2)-containing
1124 cyanobacterium (Oxyphotobacteria). *Int. J. Syst. Evol. Microbiol.* **50**: 1833-1847.

1125 Rocap, G., and others. 2003. Genome divergence in two *Prochlorococcus* ecotypes reflects
1126 oceanic niche differentiation. *Nature* **424**: 1042-1047.

1127 Sahlsten, E. 1987. Nitrogenous nutrition in the euphotic zone of the central North Pacific Gyre.
1128 *Mar. Biol.* **96**: 433-439.

1129 Saito, M. A., T. J. Goepfert, and J. T. Ritt. 2008. Some thoughts on the concept of colimitation:
1130 Three definitions and the importance of bioavailability. *Limnol. Oceanogr.* **53**: 276-290.

1131 Scanlan, D. J., and others. 2009. Ecological genomics of marine picocyanobacteria. *Microbiol.*
1132 *Mol. Biol. Rev.* **73**: 249-299.

1133 Shi, Y. M., J. McCarren, and E. F. DeLong. 2012. Transcriptional responses of surface water
1134 marinemicrobial assemblages to deep-sea water amendment. *Environ. Microbiol.* **14**:
1135 191-206.

1136 Shi, Y. M., G. W. Tyson, J. M. Eppley, and E. F. DeLong. 2011. Integrated metatranscriptomic
1137 and metagenomic analyses of stratified microbial assemblages in the open ocean. *ISME J.*
1138 **5**: 999-1013.

1139 Sohm, J. A., and others. 2016. Co-occurring *Synechococcus* ecotypes occupy four major oceanic
1140 regimes defined by temperature, macronutrients and iron. *ISME J.* **10**: 333-345.

1141 Solomon, C. M., J. L. Collier, G. M. Berg, and P. M. Glibert. 2010. Role of urea in microbial
1142 metabolism in aquatic systems: a biochemical and molecular review. *Aquat. Microb.*
1143 *Ecol.* **59**: 67-88.

1144 Sosa, O. A., S. M. Gifford, D. J. Repeta, and E. F. DeLong. 2015. High molecular weight
1145 dissolved organic matter enrichment selects for methylotrophs in dilution to extinction
1146 cultures. *ISME J.* **9**: 2725-2739.

1147 Steeman-Nielsen, E. 1952. The use of radioactive carbon (C14) for measuring organic

1148 production in the sea. *J. Cons. Int. Explor. Mer.* **18**: 117-140.

1149 Sterner, R.W. and J.J. Elser. 2002. *Ecological Stoichiometry: The Biology of Elements from*
1150 *Molecules to Biosphere*. Princeton University Press. Princeton, N.J.

1151 Stoddard, L. I., J. B. H. Martiny, and M. F. Marston. 2007. Selection and characterization of
1152 cyanophage resistance in marine *Synechococcus* strains. *Appl. Environ. Microbiol.* **73**:
1153 5516-5522.

1154 Strickland, J. D. H. and T. R. Parsons. 1972. *A practical handbook of seawater analysis*. Second
1155 Edition, Bulletin 167. Fisheries Research Board of Canada, Ottawa.

1156 Strzepek, R. F., and P. J. Harrison. 2004. Photosynthetic architecture differs in coastal and
1157 oceanic diatoms. *Nature* **431**: 689-692.

1158 Suggett, D. J., C. M. Moore, A. E. Hickman, and R. J. Geider. 2009. Interpretation of fast
1159 repetition rate (FRR) fluorescence: signatures of phytoplankton community structure
1160 versus physiological state. *Mar. Ecol.: Prog. Ser.* **376**: 1-19.

1161 Sunda, W. G., D. G. Swift, and S. A. Huntsman. 1991. Low iron requirement for growth in
1162 oceanic phytoplankton. *Nature* **351**: 55-57.

1163 Thompson, A. W., K. Huang, M. A. Saito, and S. W. Chisholm. 2011. Transcriptome response of
1164 high- and low-light-adapted *Prochlorococcus* strains to changing iron availability. *ISME*
1165 *J.* **5**: 1580-1594.

1166 Vault, D., D. Marie, R. J. Olson, and S. W. Chisholm. 1995. Growth of *Prochlorococcus*, a
1167 photosynthetic prokaryote, in the equatorial pacific-ocean. *Science* **268**: 1480-1482.

1168 Van Wambeke, F., S. Bonnet, T. Moutin, P. Raimbault, G. Alarcon, and C. Guieu. 2008. Factors
1169 limiting heterotrophic bacterial production in the southern Pacific Ocean. *Biogeosciences*
1170 **5**: 833-845.

1171 Ward, B. A., S. Dutkiewicz, C. M. Moore, and M. J. Follows. 2013. Iron, phosphorus, and
1172 nitrogen supply ratios define the biogeography of nitrogen fixation. *Limnol. Oceanogr.*
1173 **58**: 2059-2075.

1174 Waterbury, J. B., S. W. Watson, R. R. L. Guillard, and L. E. Brand. 1979. Widespread
1175 occurrence of a unicellular, marine, planktonic cyanobacterium. *Nature* **277**: 293-294.

1176 Welschmeyer, N. A. 1994. Fluorometric analysis of chlorophyll-*a* in the presence of chlorophyll-
1177 *b* and pheopigments. *Limnol. Oceanogr.* **39**: 1985-1992.

1178 Wheeler, P. A., and D. L. Kirchman. 1986. Utilization of inorganic and organic nitrogen by
1179 bacteria in marine systems. *Limnol. Oceanogr.* **31**: 998-1009.

1180 Wickham, H. 2009. *ggplot2: Elegant graphics for data analysis*. Springer-Verlag New York.

1181 Worden, A. Z., J. K. Nolan, and B. Palenik. 2004. Assessing the dynamics and ecology of marine
1182 picophytoplankton: The importance of the eukaryotic component. *Limnol. Oceanogr.* **49**:
1183 168-179.

1184 Yool, A., A. P. Martin, C. Fernandez, and D. R. Clark. 2007. The significance of nitrification for
1185 oceanic new production. *Nature* **447**: 999-1002.

1186 Zehr, J. P., and R. M. Kudela. 2011. Nitrogen cycle of the open ocean: from genes to ecosystems.
1187 *Annu. Rev. Mar. Sci.* **3**: 197-225.

1188 Zhang, J. J., K. Kobert, T. Flouri, and A. Stamatakis. 2014. PEAR: a fast and accurate Illumina
1189 Paired-End reAd mergeR. *Bioinformatics* **30**: 614-620.

1190 Zhu, Y., D. X. Yuan, Y. M. Huang, J. Ma, S. C. Feng, and K. N. Lin. 2014. A modified method
1191 for on-line determination of trace ammonium in seawater with a long-path liquid
1192 waveguide capillary cell and spectrophotometric detection. *Mar. Chem.* **162**: 114-121.

1193

1194 **Figure legends**

1195 **Figure 1.** Geographic locations in the North Pacific (a), sea surface height anomaly (b) and
1196 potential density profiles (c) of the two stations where nutrient addition experiments were
1197 conducted in August of 2014. Station 38 was in the western part of transition zone of California
1198 Current System (station TZ), and Station 52 was in the oligotrophic North Pacific Subtropical
1199 Gyre (station GY).

1200

1201 **Figure 2.** Phytoplankton community responses to N compounds and Fe at two stations in the
1202 NPSG. (a) Chlorophyll *a*, (b) rates of ¹⁴C-PP measured after 48 hrs of incubation at the GY and
1203 TZ stations. The significantly different means (t-test, n=3, p<0.05) are indicated with unique
1204 small letters where letter 'a' indicates values not-significantly different from the control. FDW:
1205 0.2 µm filtered 600 m water. The dashed lines show measurements at T0 in the control (no
1206 amendments). The dotted and dotdash lines in (b) show measurements at T0 in the N + Fe and
1207 FDW additions, respectively.

1208

1209 **Figure 3.** Phytoplankton photosystem II physiology responses to N compounds and Fe in the
1210 NPSG. (a and b) Maximum *in vivo* fluorescence yield (F_m); (c and d) maximum photochemical
1211 efficiency of PSII (F_v/F_m); (e and f) functional absorption cross-section of PSII (σ_{PSII}) measured
1212 at 470 nm (a, c, e) and 505 nm (b, d, f) excitation wavelength in response to nutrient additions at
1213 the GY and TZ stations. The dashed lines show measurements at T0 in the control (no
1214 amendments). The significantly different means (t-test, n=3, p<0.05) are indicated with unique
1215 small letters where letter 'a' indicates values not-significantly different from the control. FDW:
1216 0.2 µm filtered 600 m water.

1217 **Figure 4.** Intergroup and spatial variability among phytoplankton and bacteria in responses to N
1218 compounds and Fe additions. Cell counts for (a) *Synechococcus*, (b) *Prochlorococcus*, (c)
1219 photosynthetic picoeukaryotes (PPE), (d) high nucleic acid containing bacteria (HNA) and (e)
1220 low nucleic acid containing bacteria (LNA) for all treatments measured 48 h after nutrient
1221 additions at the GY and TZ stations. The significantly different means (t-test, n=3, p<0.05) are
1222 indicated with unique small letters where letter 'a' indicates values not-significantly different
1223 from the control. FDW: 0.2 µm filtered 600 m water.

1224

1225 **Figure 5.** Nitrogen additions resulted in a shift in microbial composition by 48 hrs in the NPSG.
1226 (a) Microbial community composition based on the relative abundance of the 16S rRNA gene
1227 copy at the genus level in the experiments at the GY and TZ stations. Only top 30 abundant
1228 genera are listed. Each sample represents a mean of 16S rRNA gene copy relative abundance
1229 from three replicates. *ua* indicates unassigned taxa. (b) PCoA on Bray-Curtis distance measures
1230 among the samples for heterotrophic microbial community composition at the GY and TZ
1231 stations.

1232

1233 **Figure 6.** Differential responses of *Prochlorococcus* oligotypes to N compounds. (a) Distinct
1234 *Prochlorococcus* communities were present at the GY (left panel) and TZ stations (right panel).
1235 Abundances of *Prochlorococcus* oligotypes, cells mL⁻¹ (Y axis), were estimated based on 16S
1236 rRNA gene amplicon sequencing, oligotyping analysis and cell counts. Oligotypes were assigned
1237 to Clade (X axis) and eStrain (legend) based on the highest nucleotide identity, where each
1238 eStrain represents a group of *Prochlorococcus* strains with 100% nucleotide identity in the V3-
1239 V4 region of the 16S rRNA gene sequence. (b) PCoA analysis on Bray-Curtis distance indices

1240 for *Prochlorococcus* community composition at T48 as a function of nutrient addition at the GY
1241 and TZ stations. (c and d) Responses in abundance of the selected *Prochlorococcus* oligotypes to
1242 nutrients at T48 at GY (c) and TZ (d). The dashed line shows abundances of each oligotype at
1243 T0.

1244

1245 **Figure 7.** Differential responses of *Synechococcus* oligotypes to N compounds. (a) Distinct
1246 *Synechococcus* communities were present at the GY (left panel) and TZ stations (right panel).
1247 Abundances of *Synechococcus* oligotypes, cells mL⁻¹ (Y axis), were estimated based on 16S
1248 rRNA gene amplicon sequencing, oligotyping analysis and cell counts. Oligotypes were assigned
1249 to Clade (X axis) and eStrain (legend) based on the highest nucleotide identity, where each
1250 eStrain represents a group of *Synechococcus* strains with 100% nucleotide identity in the V3-V4
1251 region of the 16S rRNA gene sequence. (b) PCoA analysis on Bray-Curtis distance indices for
1252 *Synechococcus* community composition at T48 as a function of nutrient addition at the GY and
1253 TZ stations. (c and d) Responses in abundance of the selected *Synechococcus* oligotypes to
1254 nutrients at T48 at the GY (c) and TZ stations (d). The dashed line shows abundances of each
1255 oligotype at T0.

Tables

Table 1. Initial conditions at the two hydrographic stations where N amendment experiments were conducted.

		GY station	TZ station
Date		8/29/14	8/24/14
Location	Latitude (ddm)	27.281	33.502
	Longitude (ddm)	-140.382	-129.37
Physics	Temperature, °C	23.84±0.01	19.50±0.04
	Salinity	35.41±0.01	33.47±0.01
Nutrients	NO ₃ ⁻ +NO ₂ ⁻ , nmol L ⁻¹	2.4±0.7	2.5±0.4
	NH ₄ ⁺ , nmol L ⁻¹ *	36±10	58±3
	SRP, μmol L ⁻¹ ***	0.094±0.005	0.272±0.005
	Si(OH) ₄ , μmol L ⁻¹ ***	1.35±0.02	2.14±0.01
	Fe, nmol L ⁻¹	below LOD ^b	below LOD ^b
Phytoplankton activity	Chl <i>a</i> , μg L ⁻¹	0.058±0.001	0.057±0.003
	¹⁴ C-PP, μmol C L ⁻¹ d ⁻¹	0.33±0.02	0.34±0.01
	Fm ₄₇₀	3.4±0.2	3.6±0.3
	Fv/Fm ₄₇₀ **	0.34±0.02	0.51±0.01
	σ _{PSII-470} × 10 ⁻²⁰ m ⁻² quanta ⁻¹	850±40	900±40
Cell abundances	Phytoplankton total, mL ⁻¹	1.6±0.5 × 10 ⁵	1.1±0.5 × 10 ⁵
	<i>Prochlorococcus</i> , mL ⁻¹	1.6±0.5 × 10 ⁵ (30.8%)	1.0±0.5 × 10 ⁵ (20.3%)
	<i>Synechococcus</i> , mL ⁻¹ *	1.2±0.8 × 10 ³ (0.2%)	3.9±0.7 × 10 ³ (0.8%)
	Photosynthetic picoeukaryotes, mL ⁻¹ *	1.14±0.03 × 10 ³ (0.2%)	2.5±0.2 × 10 ³ (0.5%)
	HNA cells, mL ⁻¹	1.2±0.1 × 10 ⁵ (23.1%)	1.3±0.2 × 10 ⁵ (25.3%)
	LNA cells, mL ⁻¹	2.4±0.2 × 10 ⁵ (46.2%)	2.6±0.3 × 10 ⁵ (53.1%)
	Total cells ^a , mL ⁻¹	5.2±0.5 × 10 ⁵	5.0±0.6 × 10 ⁵

Concentrations of nutrients are shown as an average (±standard deviation) of three replicates.

Chl *a* – chlorophyll *a* concentration; ¹⁴C-PP – primary productivity rates; HNA – high nucleic acid cells; LNA – low nucleic acid cells, Fm₄₇₀ – maximum fluorescence at 470 nm, Fv/Fm₄₇₀ – maximum photochemical efficiency of PSII measured at 470 nm, σ_{PSII-470} – functional absorption

cross-section of PSII measured at 470 nm. Significant difference in means is shown with *** for $p < 0.001$, ** for $p < 0.01$ and * for $p < 0.1$ (two-sample t-test).

^aTotal cells: *Prochlorococcus*+*Synechococcus*+Photosynthetic picoeukaryotes+HNA+LNA cells

^bFe limit of detection (LOD) was $0.058 \text{ nmol L}^{-1}$.

Table 2. Relative abundance and characteristics of *Prochlorococcus* and *Synechococcus* oligotypes at two experimental sites at the start of the incubation. The abundance is based on 16S rRNA gene copies and shown as percent of total 16S rRNA gene copies for each genus. Only oligotypes that contributed at least 1% to *Prochlorococcus* and *Synechococcus* populations at both sites are shown. Identity (%) shows percent nucleotide identity to the 16S rRNA gene of the closest strain(s). Score (bits) shows BLASTN score results. eStrain is a representative of a group of strains with 100% identical 16S rRNA gene V3-V4 region.

Oligotype ID	Nucleotides at high entropy positions	Nucleotide identity, %	eStrain	Clade	Relative abundance at GY, %	Relative abundance at TZ, %
<i>Prochlorococcus</i>						
MED4-oligo1	CGTTTCT	100	MED4	HLI	0.96	73.75
MIT9301-oligo1	TGCTAAT	100	MIT9301	HLII	66.19	0.29
MIT9312-oligo1	TACTAAT	100	MIT9312	HLII	21.64	0.45
MIT9515-oligo1	CGCTTCT	100	MIT9515	HLI	0.54	10.72
MED4-oligo2	CGTTTTT	99.75	MED4	HLI	0.55	3.75
MED4-oligo3	CGTTTAT	99.75	MED4	HLI	0.37	2.92
MIT9515-oligo2	CGCTTAT	99.75	MIT9515	HLI	0.64	1.42
SB-oligo1	TGTTAAT	100	SB	HLII	1.93	0.03
MIT9301-oligo2	TGCTTAT	99.51	MIT9301	HLII	1.91	0.04
NATL1A-oligo1	CGCTTTT	99.75	NATL1A	LLI	0.28	1.61
PAC1-oligo1	TGCTTTT	99.75	PAC1	LLI	0.85	0.76
MIT9312-oligo2	TACTTAT	99.51	MIT9312	HLII	1.26	0.01
<i>Synechococcus</i>						
CC9605-oligo1	ATACTCTATGC	100.00	CC9605	Clade II	61.12	34.93
CC9605-oligo2	ATACTCTATGT	99.75	CC9605	Clade II	25.46	14.09
CC9902-oligo1	ATACTCTAAGC	100.00	CC9902	Clade IV	0.00	26.30
CC9902-oligo2	ATACTCTAAGT	99.75	CC9902	Clade IV	0.00	13.64
KORDI100-oligo1	ATCCGCTCTGC	99.75	KORDI-100	Clade V	0.97	5.11
CC9605-oligo3	ATGCTCTATGC	99.75	CC9605	Clade II	5.77	0.00
CC9605-oligo4	ACACTCTATGC	99.75	CC9605	Clade II	4.34	0.34
CC9605-oligo5	ATACTCTCTGC	99.75	CC9605	Clade II	0.48	0.84
KORDI100-oligo2	ATCCGTTCTGT	99.26	KORDI-100	Clade V	0.00	1.10

Table 3. Responses of microbial communities to urea, NO_3^- , NH_4^+ and Fe additions in the North Pacific Ocean. The responses after 48 hrs are summarized for all N forms and specifically for each N substrate. Responses shared between the two stations are shown in grey, and responses specific for TZ and GY stations are shown in orange and blue, respectively. The arrow up (\Uparrow) shows an increase, and the arrow down (\Downarrow) shows a decrease in value. Triangle (Δ) shows a shift in community composition. Reverse triangle (∇) shows consumption of a nutrient (Table S5). The width of arrows and size of triangles reflect the magnitude of change. The empty boxes for individual substrates/elements indicate that the response was similar to that shown in column “All N substrates”. The empty boxes in the “All N substrates” indicate that the response differed among all N substrates.

Category	Measurement	All N substrates	Urea	NO ₃ ⁻	NH ₄ ⁺	Fe
Functional	Chl <i>a</i> concentrations	↑	↑		↑	↑
	¹⁴ C-PP rates	↑	↑		↑	↑
	Fm	↑	↑	↑	↑	↑
	Fv/Fm	↑	↑	↑	↑	↑
	σ _{PSII}		↓		↓	
Taxonomic I: cell count	<i>Prochlorococcus</i>	↑	↑		↑	
	<i>Synechococcus</i>		↑	↑		↑
	PPE	↑				↑
	HNA cells			↑	↑	
Taxonomic II: community composition based on 16S rRNA gene	Heterotrophic microbial community	▲		▲	▲	▲
	<i>Prochlorococcus</i>	▲	▲	▲	▲	▲
	<i>Synechococcus</i>		▲	▲	▲	
Nutrient consumption	N substrate	▼			▼	
	PO ₄ ³⁻	▼			▼	▼

Differential effects of nitrate, ammonium and urea as N sources for microbial communities in the North Pacific Ocean

Authors

¹Shilova IN^a, ²Mills MM^a, ³Robidart JC, ¹Turk-Kubo KA, ⁴Björkman KM, ¹Kolber Z, ⁵Rapp I.,
²van Dijken GL, ⁴Church MJ[†], ²Arrigo KR, ⁵Achterberg EP, ¹Zehr JP*

Figures

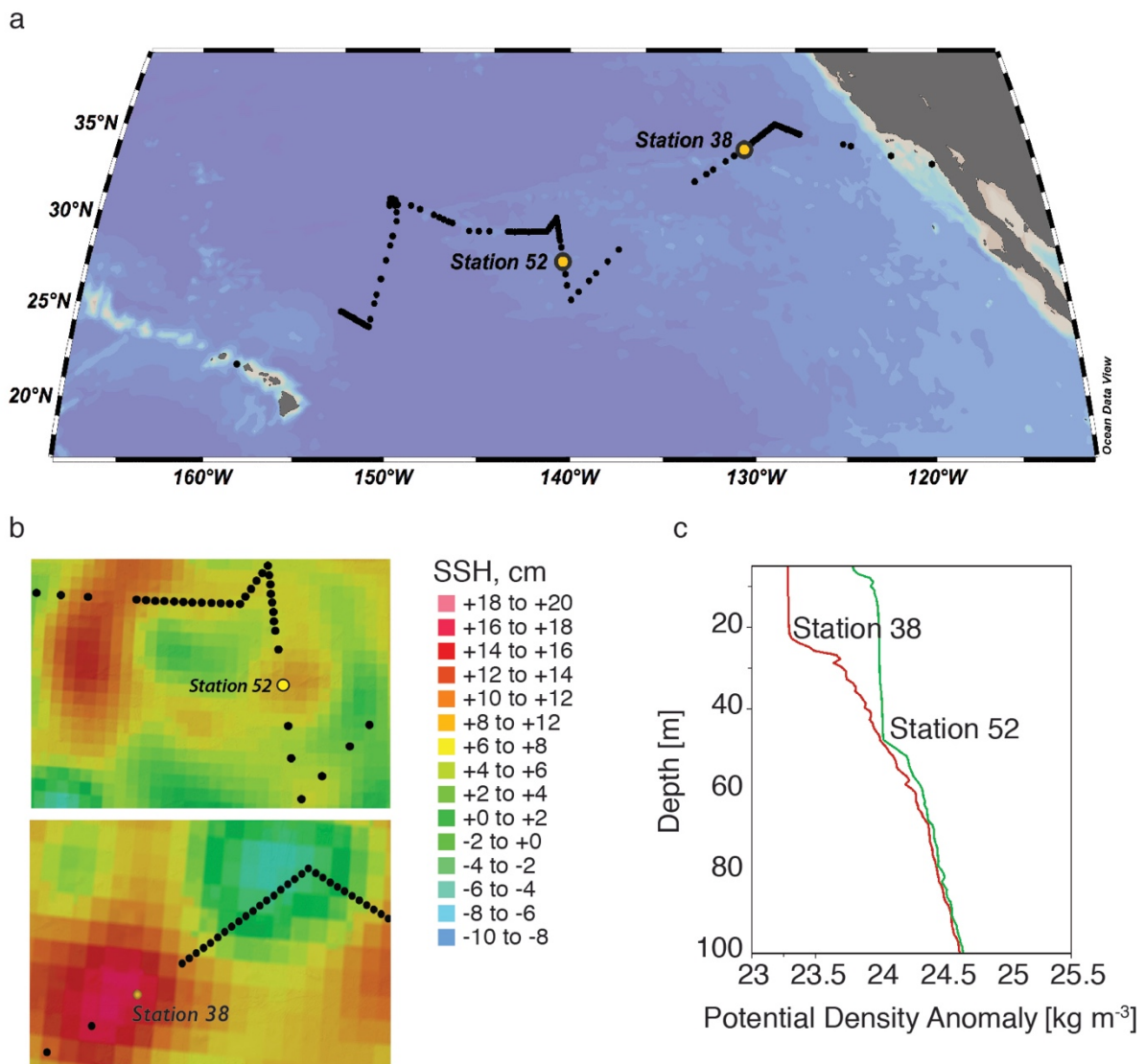


Figure 1

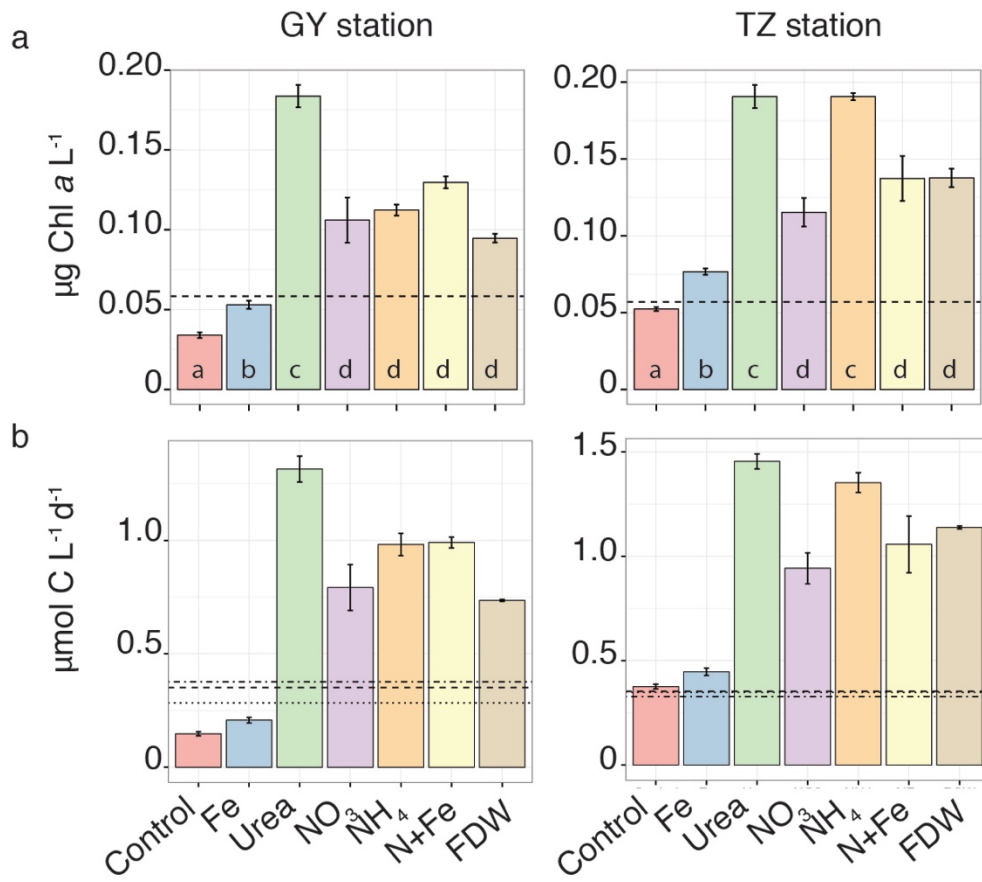


Figure 2

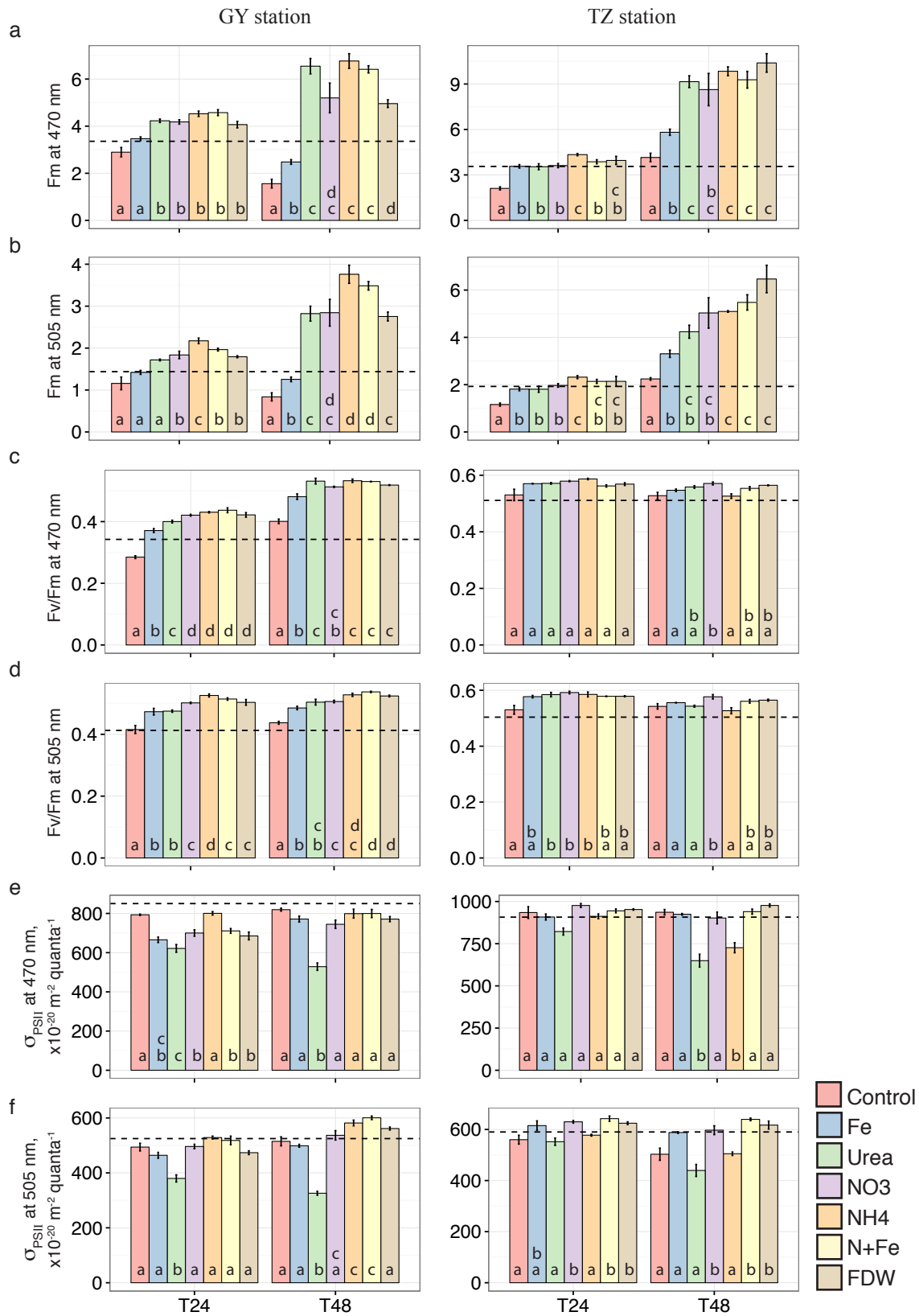


Figure 3

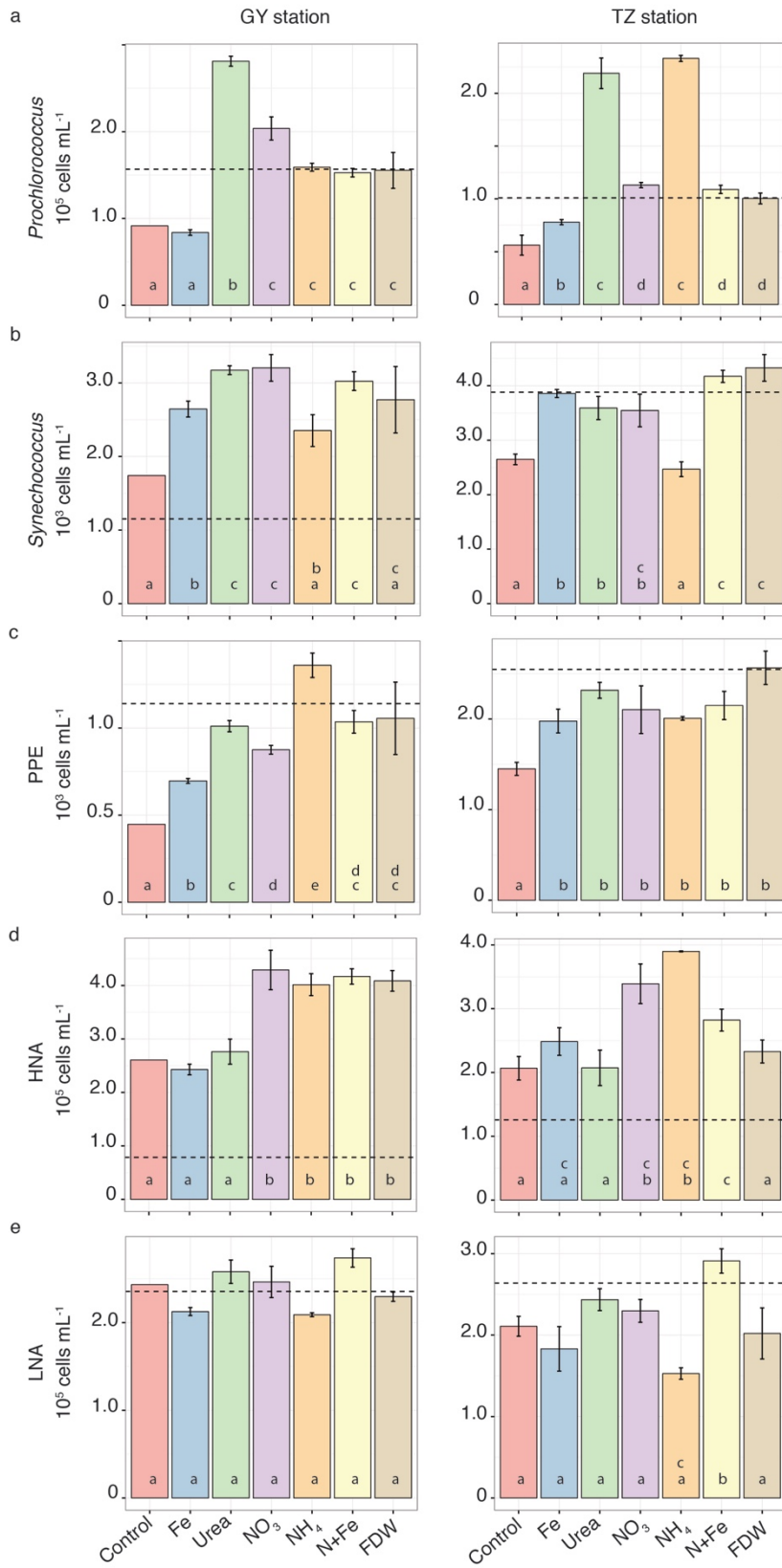


Figure 4

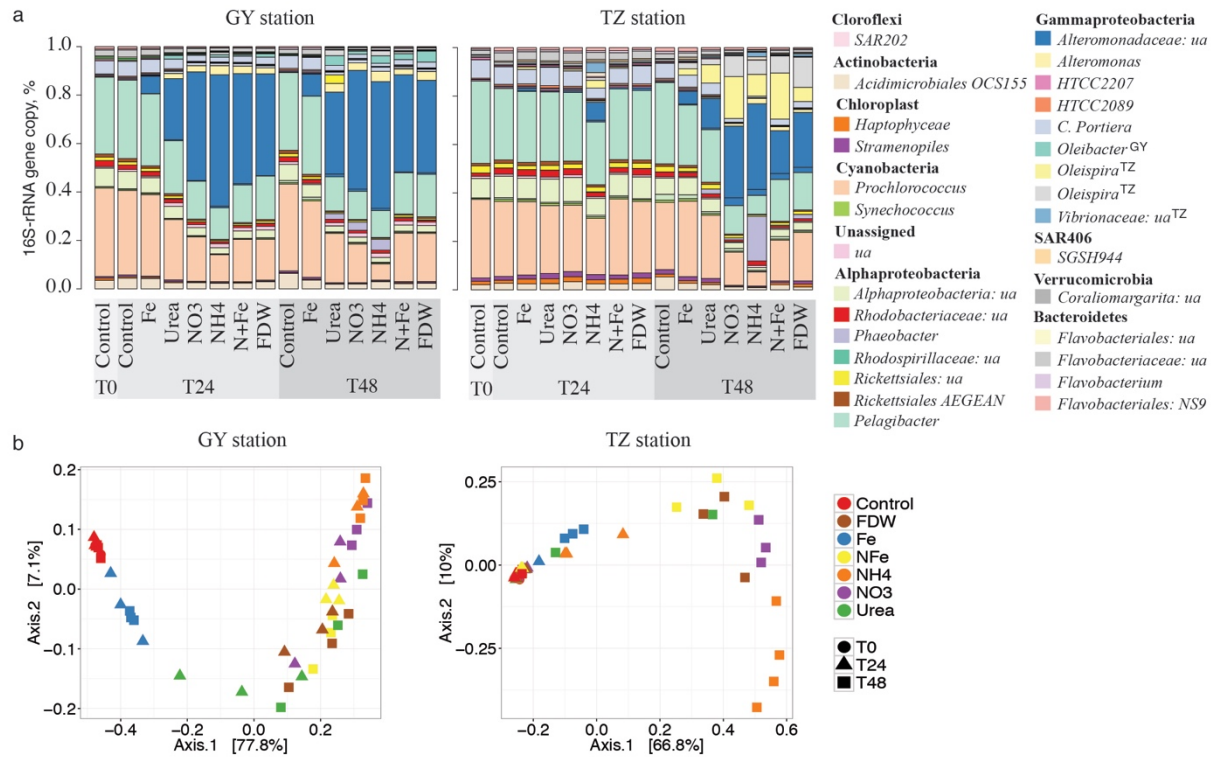


Figure 5

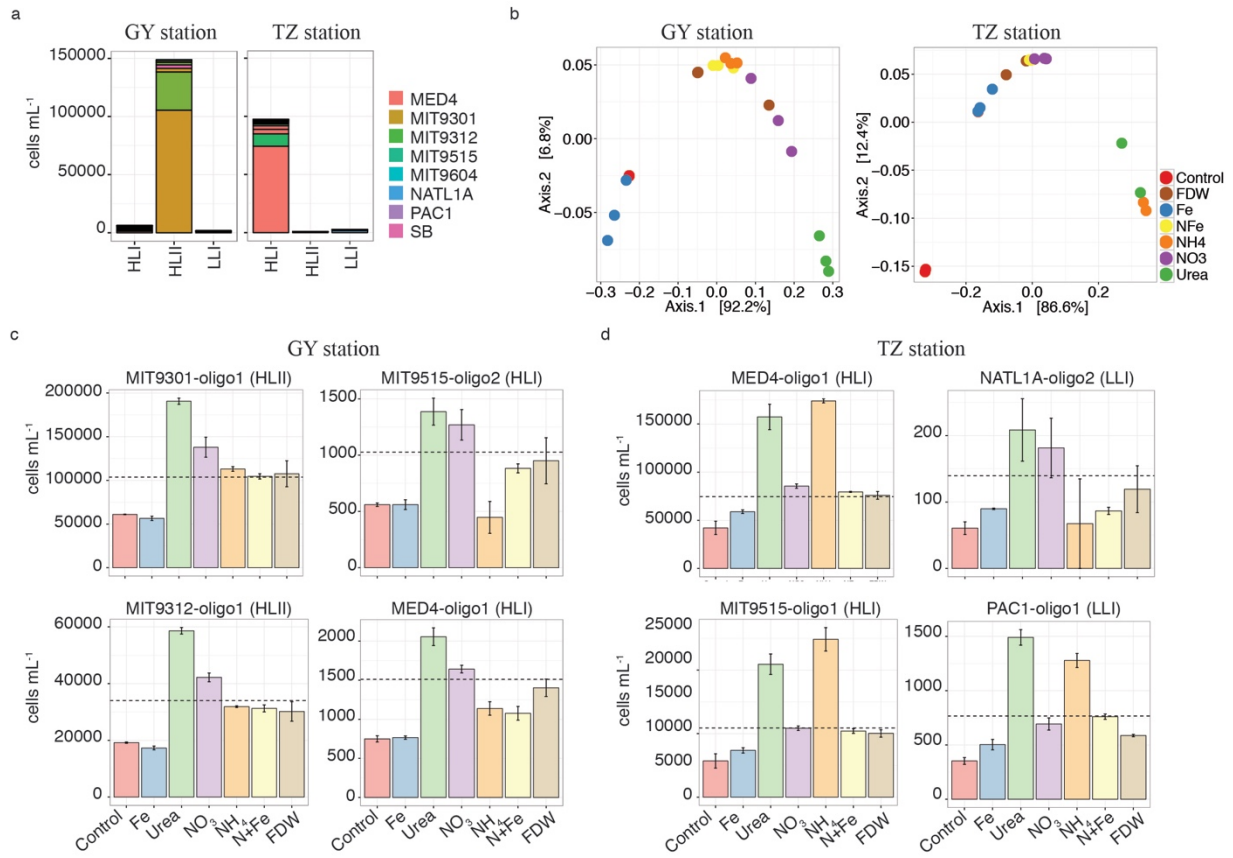


Figure 6

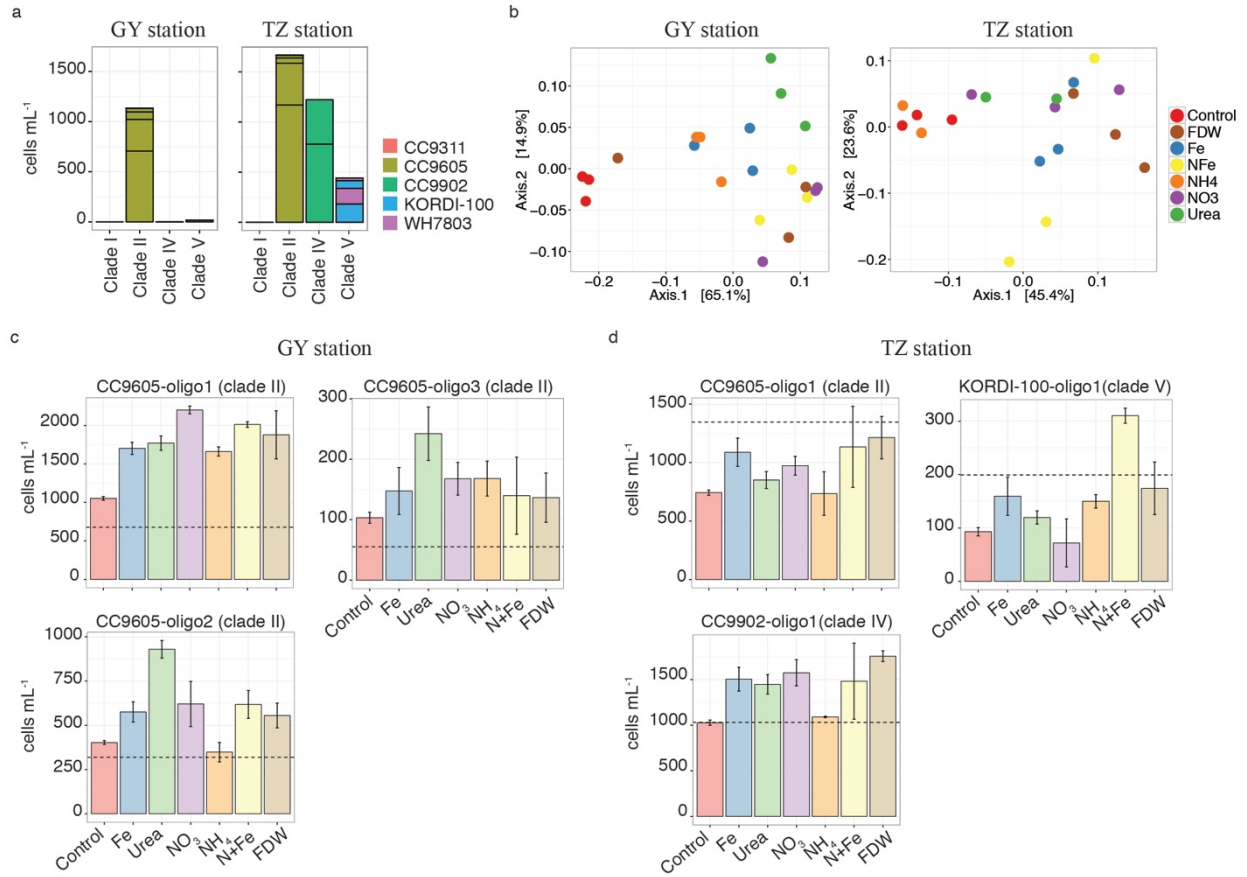


Figure 7

Title

Differential effects of nitrate, ammonium and urea as N sources for microbial communities in the North Pacific Ocean

Authors

¹Shilova IN^a, ²Mills MM^a, ³Robidart JC, ¹Turk-Kubo KA, ⁴Björkman KM, ¹Kolber Z, ⁵Rapp I.,
²van Dijken GL, ⁴Church MJ, ²Arrigo KR, ⁵Achterberg EP, ¹Zehr JP*

Supplementary Information

Table S1. Oligotypes annotation: strains with identical nucleotide sequence in the V3-V4 region of the 16S-rRNA gene were grouped into eStrains.

Organism	eStrain	Strains
<i>Prochlorococcus</i>	MED4	<i>Prochlorococcus marinus</i> str. EQPAC1
		<i>Prochlorococcus marinus</i> MED4
	MIT9301	<i>Prochlorococcus marinus</i> str. GP2
		<i>Prochlorococcus marinus</i> str. MIT 9401
		<i>Prochlorococcus marinus</i> str. MIT 9322
		<i>Prochlorococcus marinus</i> str. MIT 9321
		<i>Prochlorococcus marinus</i> str. MIT 9314
		<i>Prochlorococcus</i> sp. MIT 0604
		<i>Prochlorococcus marinus</i> str. MIT 9202
		<i>Prochlorococcus marinus</i> str. MIT 9215
		<i>Prochlorococcus marinus</i> str. MIT 9301
		<i>Prochlorococcus marinus</i> str. AS9601
		MIT9312
	<i>Prochlorococcus marinus</i> str. PAC1	
	<i>Prochlorococcus marinus</i> str. MIT 9302	
	<i>Prochlorococcus marinus</i> str. MIT 9107	
	<i>Prochlorococcus marinus</i> str. MIT 9123	
	<i>Prochlorococcus marinus</i> str. MIT 9201	
	<i>Prochlorococcus marinus</i> str. MIT 9116	
	<i>Prochlorococcus marinus</i> str. MIT 9312	
MIT9515	<i>Prochlorococcus marinus</i> str. MIT 9515	
NATL1A	<i>Prochlorococcus</i> sp. MIT 0801	
	<i>Prochlorococcus marinus</i> str. NATL1A	
	<i>Prochlorococcus marinus</i> str. MIT 9515	
PAC1	<i>Prochlorococcus marinus</i> str. PAC1	
SB	<i>Prochlorococcus marinus</i> str. SB	
<i>Synechococcus</i>	CC9311	<i>Synechococcus</i> sp. WH 8020
		<i>Synechococcus</i> sp. CC9311
	CC9605	<i>Synechococcus</i> sp. WH 8016
		<i>Synechococcus</i> sp. WH 8109
		<i>Synechococcus</i> sp. KORDI-52
		<i>Synechococcus</i> sp. WH 8103
		<i>Synechococcus</i> sp. CC9605
	CC9902	<i>Synechococcus</i> sp. BL107
		<i>Synechococcus</i> sp. CC9902
	KORDI-100	<i>Synechococcus</i> sp. KORDI-100
<i>Synechococcus</i> sp. CC9616		

Table S2. T-test statistics summary for evaluating means for chlorophyll *a* concentrations and rates of primary productivity.

Table S3. T-test statistics summary for evaluating means for FRRF parameters: F_m , F_v/F_m and σ_{PSII} .

Table S4. T-test statistics summary for evaluating means for phytoplankton and bacterial group cell counts.

Table S5. Nutrient consumption at the end of the experiments (concentrations at T0 – concentrations at T48). Percentage of nutrient utilized is shown in parenthesis. Urea concentrations were not measured.

Experiment	Treatment	N+N nmol L ⁻¹	NH ₄ ⁺ nmol L ⁻¹	SRP nmol L ⁻¹
TZ	NH ₄		2400±180 (48)	62±8 (23)
	NO ₃	1480±64 (30)		33±8 (12)
	Urea*			34±9 (13)
	NFe	470±100 (17)	5300±140 (99)	
GY	NH ₄		1360±92 (54)	27±7 (29)
	NO ₃	1040±240 (41)		36±8 (38)
	Urea*			36±15 (38)
	NFe	620±160 (28)	2040±60 (97)	33±7 (37)

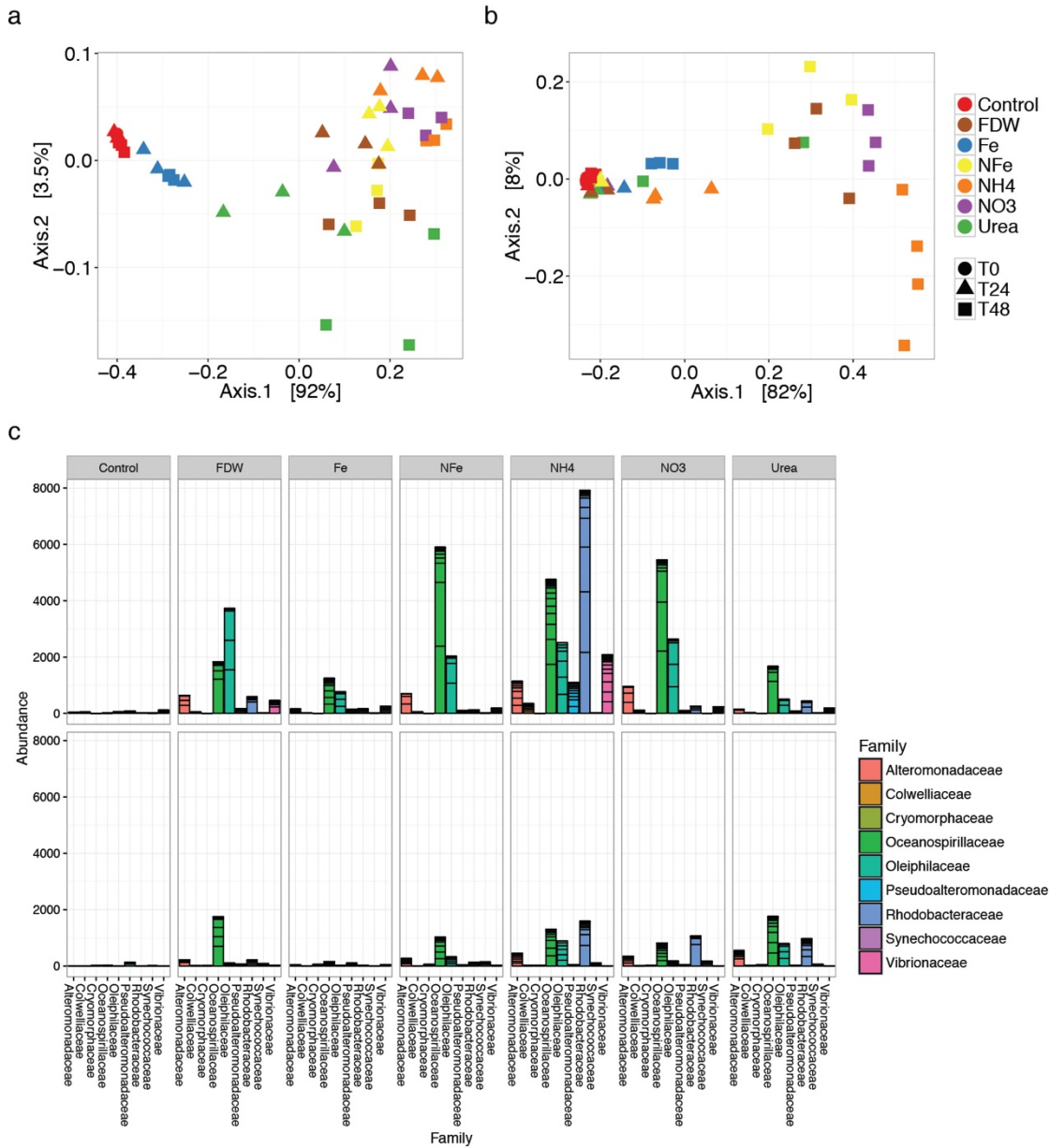


Figure S1. PCoA of heterotrophic community composition shifts in response to nutrient addition measured with the Bray-Curtis index produced similar results to the PCoA based on the Jaccard index (as shown in Fig. 5). (a) GY station, and (b) TZ station. The samples are color-coded by treatment and the shape corresponds to the time of sampling. (c) Relative abundances of 16S-rRNA sequences for most variable microbial families shown for the TZ (top panel) and GY stations (bottom panel).

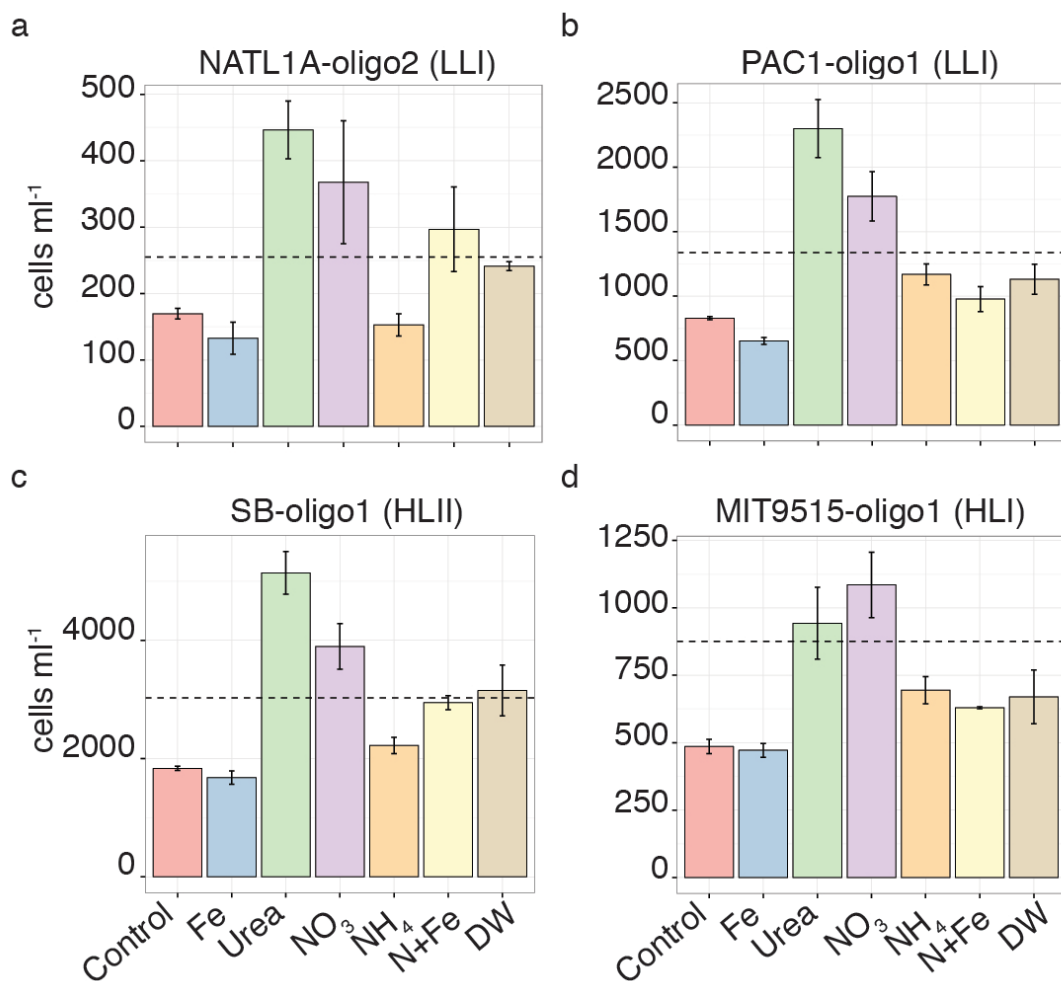


Figure S2. Differential responses of *Prochlorococcus* oligotypes to N compounds. Cell abundances of the selected *Prochlorococcus* oligotypes in response to nutrient additions after 48 of incubation at the GY station. The dashed line shows cell abundances of each oligotype at T0.